

# We are IntechOpen, the world's leading publisher of Open Access books Built by scientists, for scientists

6,900

Open access books available

186,000

International authors and editors

200M

Downloads

Our authors are among the

154

Countries delivered to

TOP 1%

most cited scientists

12.2%

Contributors from top 500 universities



WEB OF SCIENCE™

Selection of our books indexed in the Book Citation Index  
in Web of Science™ Core Collection (BKCI)

Interested in publishing with us?  
Contact [book.department@intechopen.com](mailto:book.department@intechopen.com)

Numbers displayed above are based on latest data collected.  
For more information visit [www.intechopen.com](http://www.intechopen.com)



---

## Porphyrin-Based Organophotocatalysts

---

Yingzhi Chen, Zheng-Hong Huang and  
Lu-Ning Wang

Additional information is available at the end of the chapter

<http://dx.doi.org/10.5772/intechopen.68223>

---

### Abstract

The planar geometric structure and the rich absorption feature endow porphyrins with interesting optoelectronic properties and also make it promising building blocks for supramolecular assembly. Recent advances in the photocatalytic applications of porphyrins, including homogeneous, heterogeneous photocatalysis, and photoelectrochemical solar cells are highlighted. Porphyrin photocatalysts are involved in the form of molecules, supported molecules, nanostructures, and thin film. Related rational design strategies are provided for each form with an aim to enhance the light conversion efficiency. Finally, the ongoing directions and challenges for the future development of porphyrin semiconductors in high-quality optoelectronic devices are also proposed.

**Keywords:** porphyrin, homogeneous photocatalysis, heterogeneous photocatalysis, nanostructure, photoelectrochemical solar cell

---

### 1. Introduction

Environment and energy issues have been presented as the biggest challenges facing humanity nowadays. Among the various solutions, photocatalysis is a promising approach both for photochemical energy conversion and for photochemical decontamination, hence to fulfill the sustainable energy supply and environment remediation by use of the abundant, natural sunlight [1–5]. To achieve efficient solar energy conversion, the photocatalysts are required to possess excellent light-harvesting capability, charge transfer efficiency (factors including exciton lifetime, mobility, etc.), as well as surface activity (specific surface area, ionic adsorption, etc.) [6–8]. Most research studies in photocatalysis have been concentrated on the use of inorganic semiconductors, such as  $\text{TiO}_2$  [9–11],  $\text{Fe}_2\text{O}_3$  [12–14],  $\text{ZnO}$  [15–17], and  $\text{Cu}_2\text{O}$  [17–19] which mostly suffer from inefficient light absorption and hardness. Strategies to enhance the

---

efficiency of these catalysts correlating with band engineering [20, 21], texture modification [16, 22], or configuration organization [23, 24] always involve complicated fabrication processes. All these limit their practical affordable applications. Still, much effort is needed to find other photoactive materials as alternatives for facile preparation and economical applications.

During the last decades, increasing attention has been paid to the field of semiconducting organic materials for optoelectronic applications [25–27]. One of the most important advantages concerning these organic materials is that their molecular structure and functions can be easily modulated via molecular design and tailoring. Additionally, integration of them into lightweight, large-area devices can be simply realized through solution processing at low cost. In addition, organic semiconductors, also referred to as  $\pi$ -conjugated molecules, are characterized by a delocalized  $\pi$ -electron system that makes them ideal building blocks for the fabrication of advanced functional nanomaterials and nanodevices [28–30]. As a typical representative of  $\pi$ -conjugated molecules, porphyrins are of particular interest due to some key aspects, such as their excellent light-harvesting property, p-type semiconducting behavior, ease of chemical modification, good supramolecular assembly, and film-forming features by means of either solution-based or thermal-based techniques [31–33]. Coupled with their chemical stability and flexibility, the use of porphyrin in optoelectronics has become a fast-growing research focus, and great development has been made in the field of organic solar cells (OSCs) [34, 35], organic field-effect transistors (OFETs) [36, 37], organic light-emitting diodes (OLEDs) [38, 39], even in flexible organic semiconductor devices.

As a photocatalyst, porphyrins were first used in homogenous photocatalysis [40]. The problem with it is the limited stability of porphyrin molecules and the recovery of them for successive use. Fortunately, this could be circumvented by mobilizing porphyrin molecules on solid supports or assembling them into robust nanostructures [41, 42]. Recently, more efforts have been made on the development of a semiconductor-based photoelectrochemical (PEC) water splitting device [43, 44], and thus organic photoelectrodes have aroused special attention. Relating progresses are dealt with in detail in separate sections. Before that we have a brief introduction of the relation between porphyrin molecular structure and optoelectronic properties. The use of molecular porphyrin as modification of inorganic semiconductors to achieve absorption of visible light is not covered in this chapter.

## 2. Porphyrins: structures and optoelectronic properties

In nature, porphyrin-related molecules are important photosynthetic pigments that perform the light-harvesting and charge/energy transfer functions in biological photosynthesis [45–48]. The role of porphyrins in photocatalysis is mainly related to their optical feature. As shown from the basic porphyrin ring (**Figure 1**), porphyrins are tetrapyrrole derivatives which are composed of four pyrrole subunits interconnected via  $-\text{CH}=\text{}$  bridges. The inner 16-membered ring with 18  $\pi$  electrons constitutes its electronic “heart,” which is responsible for the optical spectra. Many authors have investigated its optoelectronic properties because of simplicity. Again, molecular engineering is easily attainable by various chemical modifications to this basic ring, leading to proper tuning of the optoelectronic properties [49–51].

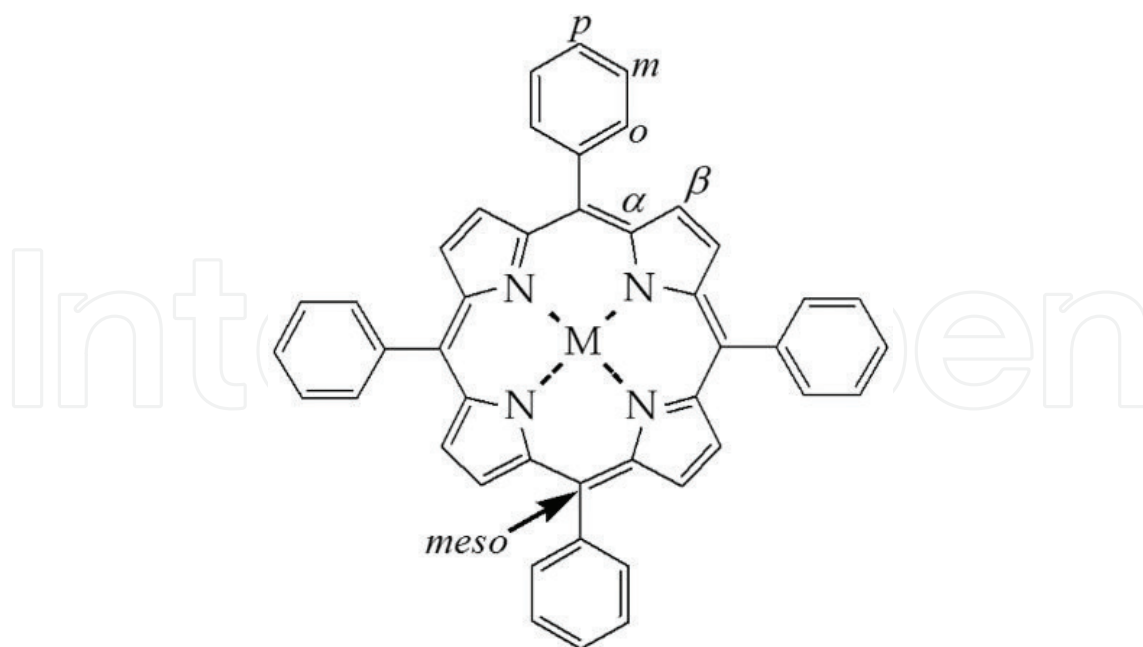


**Figure 1.** An illustration of a representative tetraarylporphyrin.

First, central substituent of porphyrin ring has a major effect on the optical spectra. Depending on the atom or group that occupies the center, porphyrins can be basically divided into free-base type (two hydrogens in the center) and metal-type [52, 53], or the so-called metalloporphyrin that is formed by exchange of the two protons in freebase porphyrin by a metal ion. Considerable varieties in the optoelectronic properties just arise from such center difference. Particularly, freebase porphyrin has a four-banded visible spectrum notably different from the two-banded spectrum exhibited by metal complex [54]. This spectral difference is attributed to the fact that the two freebase hydrogens in the center greatly reduce the symmetry from square to rectangular. In the case of metalloporphyrin [55], the change of metal in some cases can strongly influence absorption spectra. It is now known that the central metal perturbs the absorption spectra mainly through the interaction of the metal electrons with those of the ring, and sometimes the coordination type can also affect the spectra.

In addition to central substituents, peripheral substituents at various locations around the ring, including four *meso* and eight  $\beta$ -positions, can also impart different properties to a greater or lesser extent to the molecule [56–58]. Xie et al. have introduced various numbers of triphenylamine and trimethoxyphenyl groups to the *meso*-positions as electron donors, in an attempt to systematically tune the highest occupied molecular orbital-lowest unoccupied molecular orbital (HOMO-LUMO) energy levels [59]. As a photocatalyst, HOMO-LUMO bandgap determines the absorption wavelength for light-harvesting efficiency, and the suitable HOMO and LUMO levels ensure an efficient electron injection and dye regeneration process. With regard to porphyrins, the modulation of the HOMO-LUMO levels, along with the corresponding optoelectronic properties, can be simply realized through proper choice of an anchoring group to the ring. In another work, Sharma and coworkers reviewed the importance of various anchoring groups linked to either *meso* or  $\beta$ -positions in improving the light collection efficiency of dye-sensitized solar cells (DSSCs) [58]. As the most widely used

anchoring group, the position of carboxylic acid (COOH) was found to vary the performance of solar cells. Increased photocurrent was generated when the position of COOH changed from the *para* position to the *meta* position. Also in some cases, porphyrin is functionalized with donor and acceptor moieties. Upon photoexcitation, the generated exciton diffuses to the donor-acceptor interface, affording enhanced charge transfer character. Meanwhile, the enlarged electron conjugation leads to a narrowing of the optical bandgap, giving rise to broad light-absorbing dye.

### 3. Porphyrin-based homogeneous photocatalysts

Increasing emphasis has been placed on photocatalysts as an environmentally friendly process to decompose organic pollutants in contaminated water and air. It is well documented that porphyrins and metalloporphyrins have contributed a lot to photooxidation catalysis in homogeneous media.

#### 3.1. Reaction mechanisms

As for highly effective triplet-state porphyrins, two possible mechanistic pathways are involved in a photocatalytic process: energy transfer and electron transfer from the triplet excited state [60, 61]. Singlet oxygen species ( $^1\text{O}_2$ ) is commonly involved during the energy transfer process, whereas other active oxygen species such as a superoxide radical anion ( $\text{O}_2^{\bullet-}$ ) or hydroxyl radical ( $\bullet\text{OH}$ ) are essentially involved in the case of the electron transfer process. Time-resolved spectroscopic methods thus provide a powerful tool to detect the transient species derived from the photocatalyst for the study of fast reaction kinetics.

Homogeneous porphyrins are well known to generate  $^1\text{O}_2$  [40, 62–64]. For example, the triplet quantum yield of *meso*-tetra(2,6-dichloro-phenyl) porphyrin (TDCPP) was reported to be 0.995, with its corresponding singlet oxygen quantum yield around 0.98 [65]. As highly recognized, the photochemically generated singlet oxygen acts as a primary oxidant in photodegrading organic pollutants and viruses in natural water. In the case of *meso*-tetra(2,6-dichloro-3-sulfophenyl) porphyrin (TDCPPS) [66] or its iron complex (FeTDCPPS) [67] when oxidizing phenols, the main photodegradation pathway involved reaction with singlet oxygen, as suggested by the following observations: the triplet state of the porphyrins was efficiently quenched by molecular oxygen; singlet oxygen phosphorescence was detected by time-resolved measurements.

#### 3.2. Homogeneous photocatalysis

As the catalyst is dissolved, it is easy to get access to all active sites, resulting in high catalytic activities. For instance, water-soluble TDCPPS and its metal complexes were successfully used in the photodegradation of 4-chlorophenol, giving rise to the main photoproducts such as *p*-benzoquinone, whereas 2,6-dimethylphenol was transformed into 2,6-dimethylbenzoquinone [60]. The same product was obtained when 4-chlorophenol was treated

with water-soluble FeTDCPPS [68] and sodium *meso*-tetra (4-sulphonatophenyl)porphyrin (NaTPPS). Photodegradation of atrazine and ametryn by *meso*-tetra(4-sulphonatophenyl)porphyrin (TPPS) or TDCPPS resulted in a mixture of photoproducts [69]. Further examples are the photooxidation of 2,4,6-trinitrotoluene (TNT) with TPPS and its iron complex (FeTPPS) to give trinitrobenzoic acid and trinitrobenzene [70]. In most cases given above, water-soluble porphyrin derivatives are adopted, which are more suitable for practical wastewater treatment.

As another case, hydrogen production is a typical photocatalytic reaction that occurs under light irradiation. Photoinduced hydrogen production from water is regarded as an efficient and cost-effective method for the conversion and storage of solar energy. This process is usually accomplished by a system containing a photosensitizer, electron carrier, electron donor, and a catalyst. Chlorophyll and ferredoxin are the natural photosensitizer and electron carrier, while porphyrins often act as an artificial photosensitizer [71]. An example of water-soluble zinc *meso*-tetra(1-methylpyridinium-4-yl)porphyrin chloride  $[ZnTMPyP^{4+}]Cl_4$  as a photosensitizer, viologens as an electron carrier, ethylenediaminetetraacetic acid (EDTA) as an electron donor, and hydrogenase ( $H_2ase$ ) as a catalyst was provided by Qian et al. Lazarides et al. reported the use of the same  $[ZnTMPyP^{4+}]Cl_4$  as a photosensitizer, but with cobaloxime complex as a catalyst [72]. Using this system, the photocatalytic activity maintained for 20 h producing in total about 280 TON of hydrogen. In some other studies, Co, Fe, and Rh porphyrins were shown to be active as the hydrogen evolution catalysts via photoinitiation using other sensitizers [73]. Scandola and coworkers reported the efficient photochemical hydrogen evolution from 1 M pH 7 phosphate buffer by using water-soluble cationic cobalt (II) porphyrin as the catalyst, ascorbic acid as the electron donor, and  $[Ru(bpy)_3]^{2+}$  ( $bpy = 2,2'$ -bipyridine) as the photosensitizer, in achievement of TON up to 725 [74]. Kinetic studies revealed a rapid electron transfer process from  $[Ru(bpy)_3]^{2+}$  to cobalt (II) porphyrin with a calculated rate constant of  $2.3 \times 10^9 M^{-1} s^{-1}$ .

## 4. Porphyrin-based heterogeneous photocatalysts

Despite the feasibility, the homogeneous porphyrin cannot be commercialized. It has a tendency toward deactivation due to photobleaching or solvolysis by the solvent, and recovery of it from the reaction media usually constitutes another difficulty. In this case, heterogenization of porphyrins seems necessary. One possible solution is to immobilize them on organic or inorganic solid support for improved stability and easy recovery. On the other hand, nanoassembly provides another way to stabilize porphyrin molecules. The two aspects are addressed in the following sections.

### 4.1. Supported porphyrin photocatalysts

Grafting of porphyrin molecules onto a solid matrix is a useful and practical approach to carry out the reaction, since solid photocatalysts can be easily separated from the reaction medium and reused.

#### 4.1.1. Inorganic support

Easily available silica has been extensively employed as a host for porphyrins [66]. Immobilized porphyrins have been obtained by covalent link to aminoalkylated silica particles for elimination of model pollutants. Through a modified Stöber technique and thiolene polymerization, porphyrin functionalized silica microspheres have been constructed and repeatedly used for the photooxidation of 1,5-dihydroxynaphthalene (DHN) [75]. Likewise, sulfonated porphyrin has been attached to silica to photooxidize 1,5-dihydroxynaphthalene (DHN) in water [67]. Results show that this solid photocatalyst is stable and can be recycled five times without significant loss of activity. Other supports such as clay, zeolites, or layered materials are also involved to host porphyrins [76, 77]. Due to immobilization, the stability of the catalysts is thereby enhanced and the efficiency loss is reduced.

#### 4.1.2. Organic polymers as supports

To obtain a high retention, porphyrins have been included inside solid polymer backbones, which are found to impart interesting modifications on their photochemical properties [61]. For instance, anionic TPPS and its metal complex have been covalently anchored onto cationic polystyrene [78]. The resulting polymer-porphyrin system with rich ionic sites showed high activity in photokilling *Escherichiacoli* cells. In another work, porphyrin-polythiophene complex has been synthesized via electrostatic interactions, leading to a high-energy transfer process [79]. Thus, singlet oxygen could be effectively generated to kill the bacteria under white light. Biodegradable chitosan can also serve as a scaffold, as in the case of chitosan-supported metallotetraphenylporphyrin complexes [80]. Porphyrin that was covalently attached to nylon fabric was also found to be very effective against *Staphylococcus aureus* [81].

Resins are alternative supports for porphyrins due to the ease of preparation. NaTPPS has been ionically bounded at polymeric ion-exchange resin (Amberlite) toward oxidizing phenols [82]. Diffuse reflectance spectra revealed that the grafted porphyrin had an absorption feature close to the homogeneous one. Different resins such as Amberlite or 16–50 mesh have been employed to support a series of porphyrins to evaluate their activity and stability with phenols as model pollutants [83]. In all cases, the preparation is simply carried out by stirring the mixture of ion exchangers and the catalysts in an appropriate medium.

#### 4.1.3. Carbon materials as supports

Compared to energy transfer, photoinduced electron transfer (PET) by transformation of excitation energy into chemical potentials in the form of long-lived carriers is at the heart of photoenergy conversion. On a molecular level, a large number of porphyrin-based dyads or triads (porphyrin-fullerene, porphyrin-quinone) have been intentionally designed to initiate the PET process [84, 85]. For heterogenization, more consideration has been given to choice of  $\pi$ -conjugated carbon materials such as carbon nanotubes (CNTs), graphene, or  $C_3N_4$  as scaffolds. Their electron-accepting nature thus offers an opportunity to facilitate electron transfer and enhance the photoconversion efficiency [86–88]. An additional advantage is their ability to form flexible macroscopic scaffolds through different techniques such as filtration or layer-by-layer assembly.

Much efforts have been made to organize porphyrins on the semiconducting CNTs because of their unique optoelectronic properties, stability, and high surface area. Steady-state fluorescence (FL) reveals that covalently connected porphyrins function as energy-harvesting and electron-transferring antennae, while the CNTs function as electron acceptors [86, 89]. FL quenching is commonly referred to as a useful fingerprint to probe the PET process. As in the case of single-wall carbon tube-zinc porphyrin (SWCNT-ZnP) hybrids (**Figure 2A**), steady-state and time-resolved FL studies (**Figure 2B**) revealed efficient FL quenching of the singlet-excited state of zinc porphyrin with the rate constants of charge separation in the range of  $(3-6) \times 10^9 \text{ s}^{-1}$  [90]. In addition, because of increased PET, a uniform film made of CNTs-porphyrin conjugates by simple filtration displayed high light-activated antimicrobial activity toward *S. aureus* with easy recovery [91].

Graphene is known to provide high-quality two-dimensional (2D) support to increase the loading content of the photocatalysts. Regarding its large surface area, special surface activities, and layered structure, much efforts have been devoted for the preparation of nanostructured graphenes, in the form of sheets, films, or quantum dots (QDs), to promote the separation and transfer of photoinduced charge carriers [92–94]. So far, a series of papers have appeared dealing with covalent and noncovalent attachment of porphyrin to graphene. Noncovalent methods include electrostatic interactions,  $\pi$ - $\pi$  interactions, and axial coordination. For instance, graphene/zinc tetraphenylporphyrin (GR/ZnTPP) composite was facilely prepared via noncovalent interaction [95]. Note that 71% FL quenching seen with ZnTPP in the GR/ZnTPP composite clearly implied a PET process from ZnTPP to GR. With the aid of GR, improved photocurrent response was found in the GR/ZnTPP composite. Likewise, multiple-bilayered graphene oxide (GO)-porphyrin film was prepared by taking advantage of the  $\pi$ - $\pi$  and electrostatic interactions between GO sheets and porphyrin molecules, and then underwent subsequent vapor reduction to give a reduced graphene oxide (rGO)-porphyrin film [96]. The as-obtained film also showed enhanced photocurrent generation following the

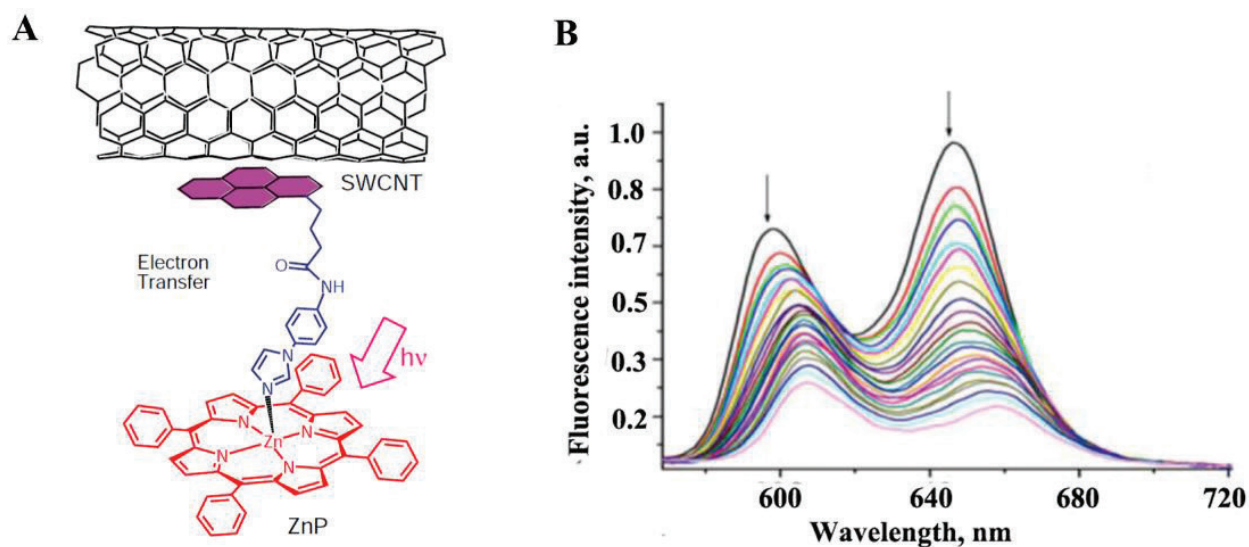


**Figure 2.** (A) Supramolecular structure of SWCNT-ZnP; (B) FL spectral changes in the visible region of ZnP during the titration of increasing addition of SWCNT, excitation wavelength  $\lambda_{\text{ex}} = 550 \text{ nm}$ . Adapted from Ref. [89].

PET. Graphene quantum dots (GQDs), have also been used to bind to zinc porphyrin by  $\pi$ - $\pi$  stacking, to give excellent photocatalytic performance toward degrading methylene blue (MB) under visible light irradiation [97].

Covalent attachment of porphyrin to graphene usually refers to the formation of covalent bonds between the different functional groups (COOH, NH<sub>2</sub>, etc.) in the periphery of the porphyrin ring and the oxygen groups of GO. By comparison with noncovalent methods, the covalent bond is stable and well defined, and moreover, the number or type of functional groups can be controlled by fine-tuning the functionalization. It is also widely accepted that the covalent band can form channels to prompt the PET between porphyrin and graphene. For instance, amine-functionalized porphyrin (TPP-NH<sub>2</sub>) and GO bound together via an amide bond (TPP-NHCO-Gr) [98]. In a different report (Figure 3), azide-terminated zinc

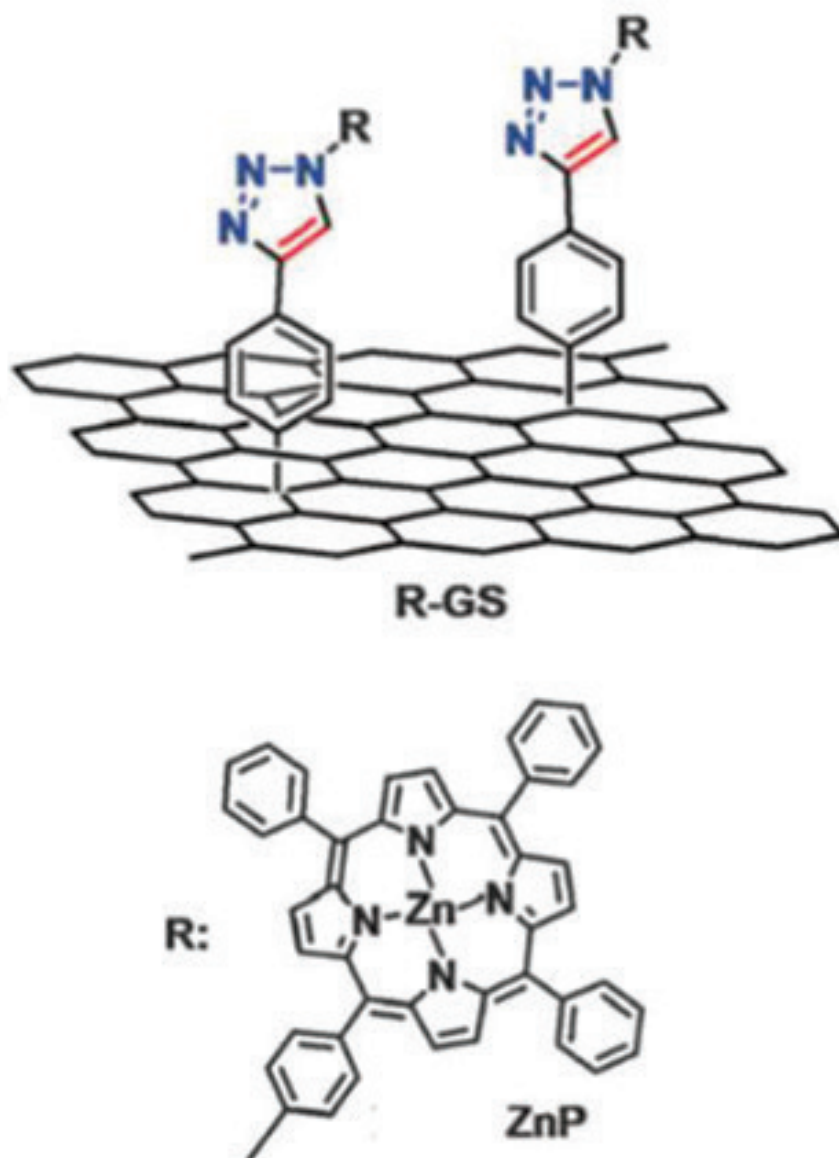


Figure 3. Schematic representation of the covalently linked ZnP-GS. Adapted from Ref. [99].

porphyrin (ZnP) and 4-(trimethylsilyl)ethynylaniline modified graphene sheets (GSs) were covalently linked to give ZnP-GS with the formation of the triazole bond [99]. Occurrence of PET was indicated in this covalently linked ZnP-GS composite based on its higher photocurrent response. Further examples are the use of different metal ions (such as  $K^+$ ,  $Ca^{2+}$ ,  $Zn^{2+}$ ,  $Cu^{2+}$ , and  $Co^{2+}$ ) as interfacial linkers to construct a series of composites between GO and 5,15-diphenyl-10,20-di(4-pyridyl)porphyrin (DPyP) [100]. The resulting strong interaction between metal ions and DPyP/GO thus facilitates the spatial separation of photogenerated charges, thereby leading to higher photocatalytic activity for hydrogen production.

Graphitic-like  $C_3N_4$  ( $g-C_3N_4$ ), as another 2D framework, is highly identified as a visible light-active polymeric semiconductor with a bandgap of  $\sim 2.7$  eV and appropriate energy levels that can extract hydrogen from water [101–104]. It is expected that  $g-C_3N_4$  can bind to porphyrin through  $\pi$ - $\pi$  stacking, electrostatic interaction, or covalent bonding, which resembles graphene. An extra merit lies in the well-matched band structures between porphyrin and  $C_3N_4$  that allow a good combination of them for increased PET. For instance, Cu (II) *meso*-tetra(4-carboxyphenyl)porphyrin (CuTCPP) was easily assembled on  $g-C_3N_4$  to form CuTCPP/ $g-C_3N_4$  composites through  $\pi$ - $\pi$  stacking interaction [88]. Given that the LUMO band of CuTCPP lies below that of  $g-C_3N_4$ , the photoinduced electrons from excited CuTCPP can be directly transferred to  $g-C_3N_4$ . This thereby reduced the probability of charge recombination, resulting in higher photocatalytic activity for phenol degradation than individual component. Natural metalloporphyrin, hemin, has been coupled with imidazole-functionalized  $g-C_3N_4$  through an axial coordination. The strong coordinate bond endowed the  $g-C_3N_4$ -hemin catalyst with enhanced stability. The obtained  $g-C_3N_4$ -hemin thus displayed higher and sustained photocatalytic oxidation activity for the degradation of 4-chlorophenol over a wide pH range [105]. In a different report, Co (II) porphyrin has been covalently linked to  $g-C_3N_4$  for photocatalytic reduction of  $CO_2$  [106]. The as-obtained hybrid possessed thirteen-fold higher photocatalytic activity ( $17 \mu\text{mol g}^{-1} \text{h}^{-1}$ ) than pure  $g-C_3N_4$  ( $1.4 \mu\text{mol g}^{-1} \text{h}^{-1}$ ). Such enhancement was attributed to the increased charge separation and prolonged lifetime of the excited state due to the electron trap by Co (II) sites.

## 4.2. Nanostructured porphyrin photocatalysts

Nanostructured porphyrins are expected to have chemical activities and stability quite different from those free or supported porphyrins [107, 108]. Particularly, the synthetic versatility enables the controllable organization of porphyrins into well-defined nanostructures via rational assembly [109–111]. For the past decade, reports began to appear on the synthesis of porphyrin nanomaterials or nanocomposites for enhanced photocatalytic performance [112–114].

### 4.2.1. Supramolecular assembly

Supramolecular assembly is defined as large aggregation of molecules held together by non-covalent bonds, such as hydrogen bonds, metal coordination, van der Waals, and  $\pi$ - $\pi$  interaction. By carefully adjusting these intermolecular interactions, aggregates with diversity and complexity can be formed [115]. For instance,  $\pi$ - $\pi$  interaction is thought to drive the

formation of nanorods of 5,15-bis(3,5-di-tert-butylphenyl)porphyrin ( $H_2DBuPP$ ) [113]. The much broader absorption in the visible and near infrared regions suggested the strong supramolecular  $\pi$ - $\pi$  interaction. As a consequence, the organized rod-crystals exhibited a broad photoresponse in the visible region (an incident photon to current conversion efficiency (IPCE):  $\sim 5.5\%$  at 460 nm), which paralleled their corresponding absorption features. As is also shown, change of the substituents at *meso*-positions to control the intermolecular interaction finally led to some difference in the length of the rod crystals.

In a different report, highly crystalline rectangular nanotubes of *meso*-tetra(4-pyridyl)porphyrin ( $H_2TPyP$ ) were synthesized [111]. The key driving forces included: hydrogen-bonding interactions along the *c*-axis, hydrogen-bonding and  $\pi$ - $\pi$  interactions along the *a*-axis, and hydrogen-bonding and hydrogen- $\pi$  intermolecular interactions along the *b*-axis, respectively. In addition, metal coordination interactions are always involved in the design of well-defined porous metal-organic frameworks (MOFs). An example is the mediation of  $Zn^{2+}$  in the assembly of *meso*-tetra(4-carboxyphenyl)porphyrin (TCPP) in **Figure 4** [116]. The X-ray diffraction (XRD) patterns of  $Zn^{2+}$ -mediated TCPP nanocubes, nanorods, and microrods are totally different from TCPP starting materials, which means that coordination bonds play a significant role in the structural change of TCPP. In another study, the involvement of  $Cu^{2+}$  has led to the assembly TCPP into 2D crystalline nanofilms [117].

All suggest that we are able to manipulate the intermolecular interactions by properly modifying the peripheral position or ring cavity of the porphyrins, thereby allowing fine-tuning of the molecular packing mode. Such a strategy enables us to construct a rich variety of nanostructures with different sizes and shapes. To date, comprehensive studies have been

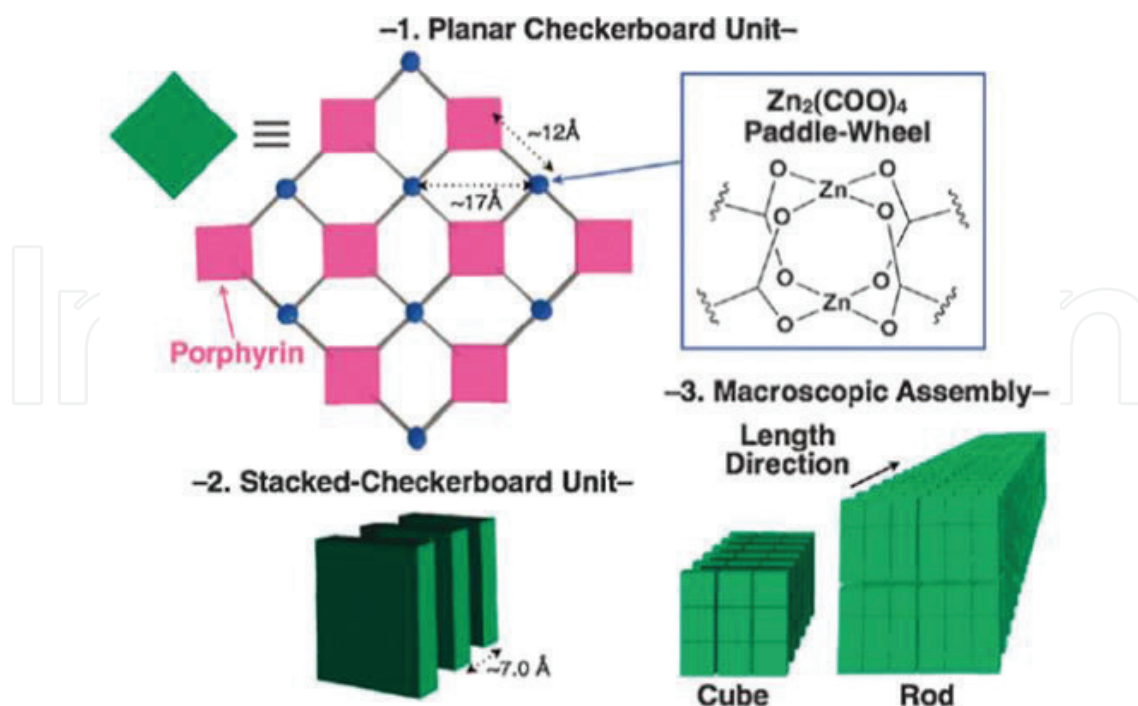


**Figure 4.** A schematic illustration of the proposed structures of TCPP architectures via paddle-wheel complexes in this study. Adapted from Ref. [116].

conducted on the preparation of porphyrin nanostructures by different synthetic methods, with morphologies varying from nanoparticles to nanowires, nanofibers, nanobelts, nanotubes, nanowheels, or films.

#### 4.2.2. Preparation and applicability

Reprecipitation is the most widely used method for supramolecular assembly. It is performed by injection of a small amount of concentrated solution of porphyrin in good solvent into a pool of poor solvent. Sometimes, addition of surfactants affords a better control of the assembly process. The aforementioned H<sub>2</sub>DBuPP nanorods were prepared by mixing of the toluene solution of H<sub>2</sub>DBuPP with nine times volume of acetonitrile [113]. The same procedure was followed to synthesize zinc *meso*-tetra(4-pyridyl)porphyrin (ZnTPyP) nanostructures [118], with the assistance of cetyltrimethylammonium bromide (CTAB) as a surfactant to control the growth. Morphologies varied from nanoparticles to nanofibers by adjusting the concentration of the surfactant or the aging time. Compared to ZnTPyP nanoparticles, the fiber-crystals demonstrated a higher photocatalytic activity toward degrading rhodamine B (RhB) pollutants. More importantly, ZnTPyP nanofibers retained the photocatalytic efficiency after eight repeated runs because of the geometric constraint. By changing the poor/good solvents, ZnTPyP hexagonal nanocylinders are obtained [119]. The internal cavity thus enabled the encapsulation of Pt-colloids-deposited TiO<sub>2</sub> nanoparticles (Pt/TiO<sub>2</sub>) to produce the final Pt/TiO<sub>2</sub>-ZnTPyP nanorods. The as-obtained nanorods showed the photocatalytic hydrogen evolution efficiency of 2 orders magnitude greater than the simple mixture of Pt/TiO<sub>2</sub> + ZnTPyP/Pt.

Different morphologies of ZnTPyP can also be synthesized through acid-base neutralization. In one study, the acidified ZnTPyP (ZnTPyP-H<sub>4</sub><sup>+</sup>) aqueous solution was mixed with the basic surfactant solution under vigorous stirring [120]. By increasing the surfactant concentration, a series of morphologies from amorphous nanoparticles to crystalline nanodisks, tetragonal nanorods, and hexagonal nanorods were synthesized with controlled size and dimension (**Figure 5A–H**). The largest pore surface area of about 457 m<sup>2</sup> g<sup>-1</sup> made porous nanodisks the most efficient catalyst in photodegrading methyl orange (MO) (**Figure 5I and J**). Moreover, the efficiency loss was greatly reduced during the repeated use due to the crystalline nature of nanodisks (**Figure 5K**). In a different report, ZnTPyP nanooctahedra were synthesized by metallization of H<sub>2</sub>TPyP [121]. In detail, Zn<sup>2+</sup> was first mixed into H<sub>2</sub>TPyP acidic aqueous solution, and the mixture was then injected into the basic solution with CTAB. Metalation of H<sub>2</sub>TPyP to ZnTPyP just took place during the acid-base neutralization, and it was observed that the morphology of ZnTPyP transformed from nanooctahedra to nanowires with increasing the pH value of the basic solution. ZnTPyP nanowires were found to have the best catalytic activity in photodegradation of MO and showed no sign of corrosion in the structure after 15 cycles. Acid-base neutralization was also used to synthesize various isolated TCPP aggregated structures, including spheres, rods, flakes, and flowers for photodegradation of RhB [122]. Graphene-supported TCPP nanorods have been synthesized to eliminate RhB by adding the basic suspension of TCPP-adsorbed graphene into acid aqueous solution of CTAB [123].

Ionic self-assembly is an attractive synthetic method that is managed by electrostatic interactions of two oppositely charged building blocks. The cooperative interactions between the

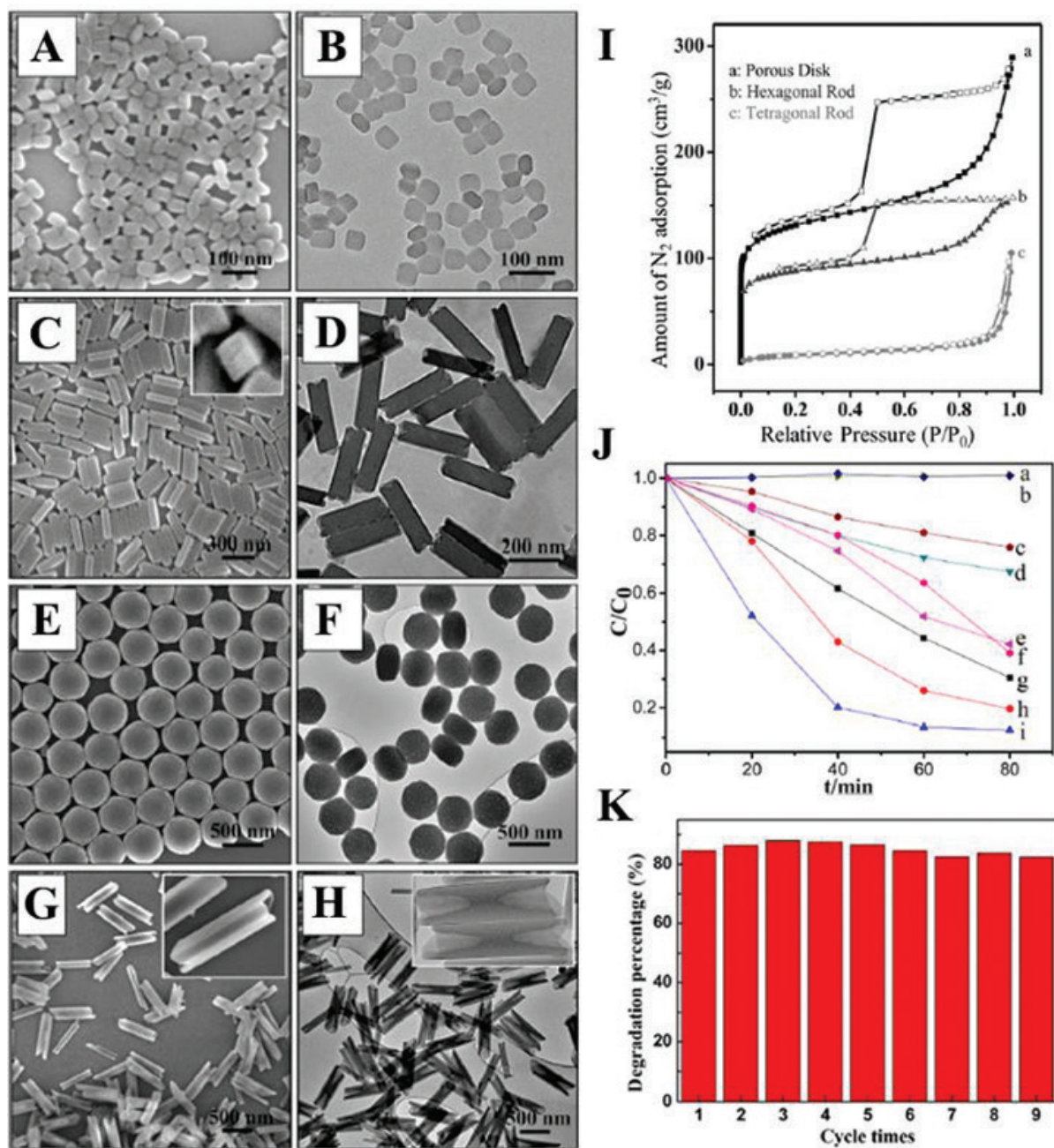


**Figure 5.** (A–H) Representative SEM images (first column), TEM images (second column) of ZnTPyP nanostructures with different morphologies: nanoparticles (A and B), tetragonal nanorods (C and D), hexagonal porous nanodisks (E and F), and hexagonal nanorods (G and H). (I) Nitrogen sorption isotherms obtained at 77 K for different ZnTPyP nanocrystals. (J) Photocatalytic activities of ZnTPyP nanocrystals. Tetragonal nanorods with 200 nm length (c), same concentration ZnTPyP in DMF (d), same concentration ZnTPyP in 0.01 M HCl (e), nanoparticles with 80 nm diameter (f), hexagonal nanowires with 2  $\mu m$  length (g), hexagonal rods with 400 nm length (h), and hexagonal porous nanodisks (i) for photo degradation of MO molecules under visible light irradiation. The results from blank experiments, where no ZnTPyP nanocrystals were used (a) an commercial P25 (b) was used are also presented for comparison. (K) Cycling tests of photocatalytic activity of ZnTPyP nanodisks under visible light irradiation. Adapted from Ref. [120].

functional subunits may afford new interesting collective properties. For instance, four-leaf clover-like morphologies have been constructed by ionic self-assembly of Zn(II) *meso*-tetra(4-sulfonatophenyl)porphyrin (ZnTPPS) and Sn(IV) *meso*-tetra(N-2-hydroxyethyl-4-pyridinium)

porphyrin (SnT(N-EtOH-4-Py)P) [124]. With Pt as the cocatalyst for hydrogen evolution, the clovers demonstrated a photoactivity far better than the sum of their individual effects. In another study, ionic assembly between tin (IV) porphyrin cation and phosphomolybdate anion led to the formation of new porphyrin-polyoxometalate hybrid nanoparticles [125]. Due to the broadened absorption and efficient electron transfer, the formed hybrid exhibited a strikingly high activity in photocatalytic hydrogen production.

Besides all that vaporization-condensation-recrystallization (VCR) organization is a commonly used way to synthesized single crystals, as in the case of H<sub>2</sub>TPyP rectangular nanotubes [111] and the tetraphenylporphyrin (H<sub>2</sub>TPP) nanoplates [126].

#### 4.2.3. Photocatalytic efficiency

A photocatalysis event usually follows three steps: exciton formation by light absorption, charge separation, and carrier conduction. Achievement of high photoenergy conversion just relies on improving the efficiency of each step. First, aggregate formation has a strong effect on the light-harvesting efficiency. As mentioned above, the aggregation of porphyrins often arises from a long-range noncovalent interaction, while the molecular arrangement into J-aggregation (relative to H-aggregation) is crucial to the light-harvesting efficiency [127]. J-aggregates are formed with a large number of molecular building blocks arranged in one dimension. The strong intermolecular  $\pi$  electronic coupling within the long axes results in a coherent excitation at red-shifted wavelengths of increasing sharpness (higher absorption coefficient). For instance, the time-dependent UV-vis spectra in monitoring the growth of one-dimensional (1D) ZnTPyP hollow hexagonal nanoprisms showed that the high-energy Soret band at 424 nm, associated with monomeric ZnTPyP, gradually decreased, with an increasing high-energy Soret band at 460 nm is associated with J-aggregated ZnTPyP [108]. The same spectral change was seen with ZnTPyP nanofibers, making the 1D nanofibers more efficient light-harvesting antenna than zero-dimensional (0D) nanoparticles [118]. On the other hand, J-aggregates are promising building blocks to direct electron transport, thereby to retard the charge recombination by stabilizing the electron transfer products. Insight into dynamics and mobility of excitons has been obtained from J-aggregates of perylene bisimides (PBIs) by transient absorption spectra [128]. The findings indicated that exciton mobility in the J-aggregates of PBIs was restricted to one dimension and exciton diffusion length was about 10 times larger than in disordered polymers. The 1D mobility thus allows for electron migration along a preferential direction without trapping effects. As proved in the case of TCPP series, J-aggregated rods exhibited more photocatalytic efficiency than the flakes and flowers [122]. As a step forward, it is proposed that alignment of the 1D nanostructures into highly ordered arrays may produce collective behavior to achieve high performance.

It is highly acknowledged that organic materials suffer from notoriously low charge carrier mobility, and photoexcited charge carriers may easily recombine before being exploited. To address it, single-crystalline organic nanostructures have been sought because the low-defect structure can largely impede the recombination of the excitons and accelerate effective charge transport. Previous reports have studied the effect of impurities on the mobility of organic pentacene, and concluded that a mobility of  $\mu = 35 \text{ cm}^2 \text{ V}^{-1} \text{ s}^{-1}$  at room temperature was increased to  $\mu = 58 \text{ cm}^2 \text{ V}^{-1} \text{ s}^{-1}$  at 225 K for pentacene single crystals [129]. Moreover, purified

rubrene single crystals have showed a maximum transistor mobility of  $\mu = 18 \text{ cm}^2 \text{ V}^{-1} \text{ s}^{-1}$  [130]. Motivated by these, growing emphasis has been placed on the synthesis of photocatalytic crystals. For instance, hierarchical structured nanocrystals of Sn (IV) *meso*-tetraphenylporphyrin dichloride (SnTPPCL) were synthesized and displayed high photocatalytic activities in the reduction of platinum nanoparticles and in photodegradation of MO [131]. The XRD patterns of SnTPPCL octahedra were indexed as a tetragonal space group, while the photocatalytic ZnTPyP rectangular nanorods were indexed as a monoclinic space group [120]. In view of the perfect molecular alignment, the photocatalytic crystals are more efficient and stable compared to the amorphous nanostructures.

Interfacial heterostructuring is another strategy to effectively reduce the recombination of photoexcited electron-hole pairs. The built-in energy level offset within the heterojunction can drive the exciton to dissociate for ready charge transfer. We have succeeded in the fabrication of 1D organic single-crystal p/n nanoheterojunctions made of p-type  $\text{H}_2\text{TPP}$  and n-type N,N-(dicyclohexyl) perylene-3,4,9,10-tetracarboxylic diimide (CH-PTCDI), as shown in **Figure 6A** and **B** [126]. The large donor-acceptor interface provides a strong driving force to separate the spatial charges, and meanwhile the 1D structure facilitates the directed charge transport along the long-range axes, thereby leading to enhanced charge separation efficiency. An efficient PET process was evidenced by the significant FL quench of CH-PTCDI when coupled with  $\text{H}_2\text{TPP}$  (**Figure 6C**). As a consequence, the  $\text{H}_2\text{TPP}/\text{CH-PTCDI}$  junction showed a remarkably high photoactivity in photodegrading MB (**Figure 6D**). It is also known that porphyrin nanostructures are able to photocatalytically reduce metal ions, which encourages the preparation of serial porphyrin/metal nanohybrids. In particular, when photocatalytic hydrogen evolution is discussed, self-platinized porphyrins are preferred, with Pt nanoparticles as cocatalysts to converted water into hydrogen gas. Examples are the self-platinized porphyrin nanotubes, nanosheets, nanofibers, and clovers that have been successfully synthesized for efficient hydrogen production [124, 132]. Additionally, a few reports have presented the combination of porphyrins with inorganic semiconductors as an exciting alternative. Such heterojunctions can take advantage of the two different material classes by allowing for a good combination of the wide absorption spectrum of porphyrins and the high mobility of the inorganic semiconductors. In one work, porphyrin- $\text{TiO}_2$  core-shell nanoparticles have been prepared and exhibit better MB photodegradation than molecular porphyrin sensitized  $\text{TiO}_2$  [133]. We also brought together the two materials to give a new configuration of  $\text{TiO}_2$  nanotube/ $\text{H}_2\text{TPP}$  nanoparticle hybrids for PEC water splitting [134]. The resulting hybrid displayed an intensive and broad absorption spectrum across 350–660 nm. Upon photoexcitation of  $\text{H}_2\text{TPP}$ , ultrafast charge injection from the excited  $\text{H}_2\text{TPP}$  into  $\text{TiO}_2$  took place, and the transferred electrons were then transported away via the unidirectional electron channels of  $\text{TiO}_2$  nanotube arrays. The increased charge separation was well proved by the largely reduced photocharge transfer resistance. Further example was provided by the aforementioned three-component Pt/ $\text{TiO}_2$ -ZnTPyP nanorods [119]. The formed electron transfer cascade from excited ZnTPyP to the conduction band of  $\text{TiO}_2$ , then to the surface of Pt nanoparticles, resulted in an enhanced hydrogen evolution efficiency. As mentioned above, the  $\pi$ -conjugated carbon materials have been established as an ideal scaffold to anchor

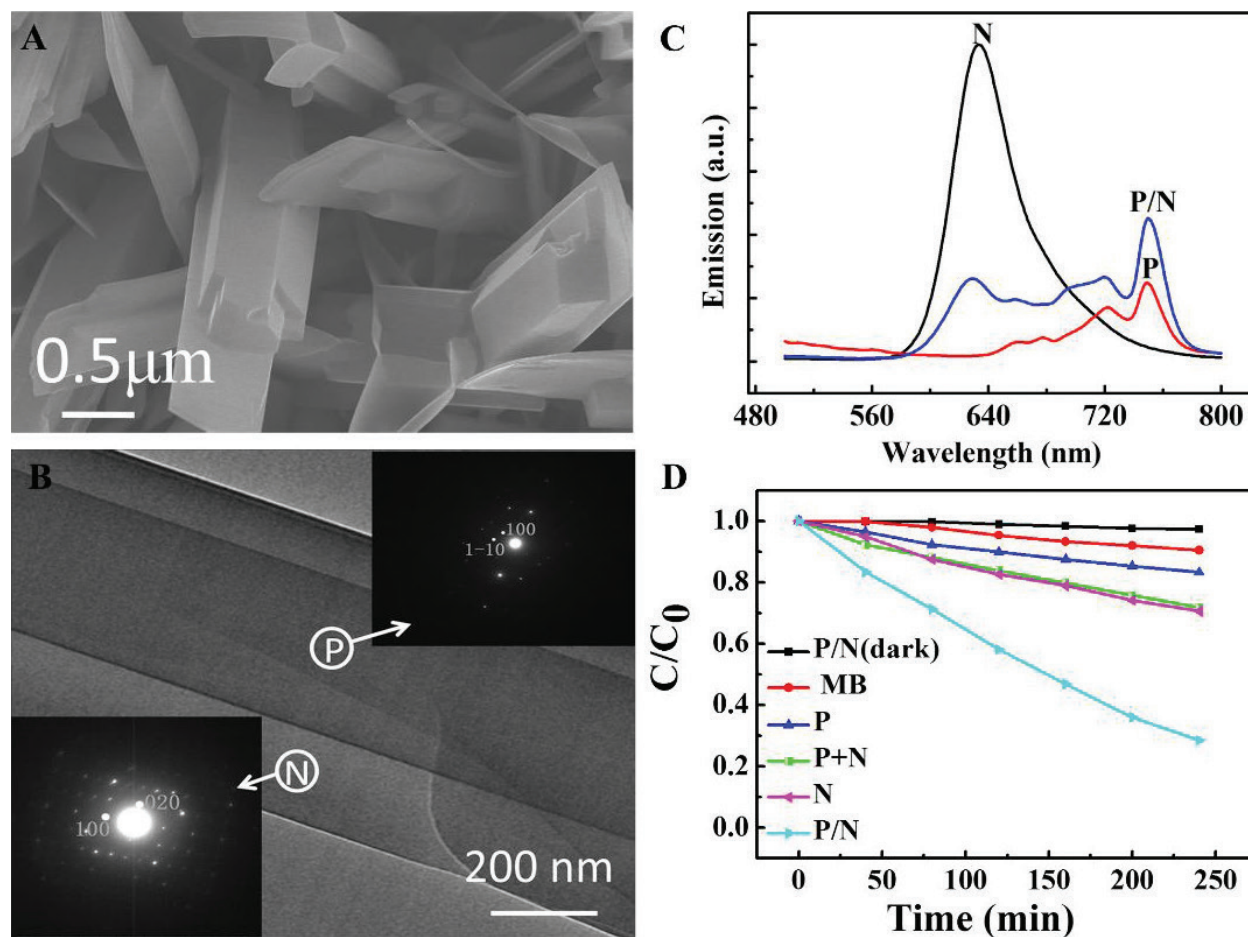


**Figure 6.** (A and B) SEM and TEM images of  $H_2TPP/CH-PTCDI$  nanoheterojunctions; (C) FL spectra of  $H_2TPP$  (P),  $CH-PTCDI$  (N), and  $H_2TPP/CH-PTCDI$  (p/n) nanostructures; (D) photocatalytic degradation of MB with different samples under visible light irradiation ( $\lambda > 400$  nm). Adapted from Ref. [125].

molecular porphyrins for stability and recyclability. Inclusion of porphyrin nanostructures into these scaffolds may seem as a logic step forward by further increasing the loading content and stability. Certainly, such combination benefits much from the increased lifetime of the charge carriers since these  $\pi$ -conjugated carbon nanostructures can serve as an excellent electron acceptor and an electron transporter as well. We have integrated  $H_2TPP$  nanoparticles into graphene for the formation of free-standing  $H_2TPP/rGO$  nanohybrid film, as shown in **Figure 7A** [135]. By coupling, the average lifetime of  $H_2TPP$  emission was lengthened from ca. 362 to 473 ps (**Figure 7B**), while the photocharge transfer was reduced from 176.2 to 46.7  $\Omega$  (**Figure 7C**). The increased electron transfer thus accounted for the improved photocatalytic performance (**Figure 7D**). For the same purpose, well-dispersed TCPP nanorods [123] or ZnTPyP nanoassemblies have been successfully fabricated on the surface of graphene nanoplates [136]. The same role was also addressed in  $g-C_3N_4$ . In this respect, a combination of  $g-C_3N_4$  and m-oxo dimeric iron (III) porphyrin ( $(FeTPP)_2O$ ) was sketched to form  $g-C_3N_4/(FeTPP)_2O$  nanocomposites, which showed dramatically improved photocatalytic hydrogen production [137].

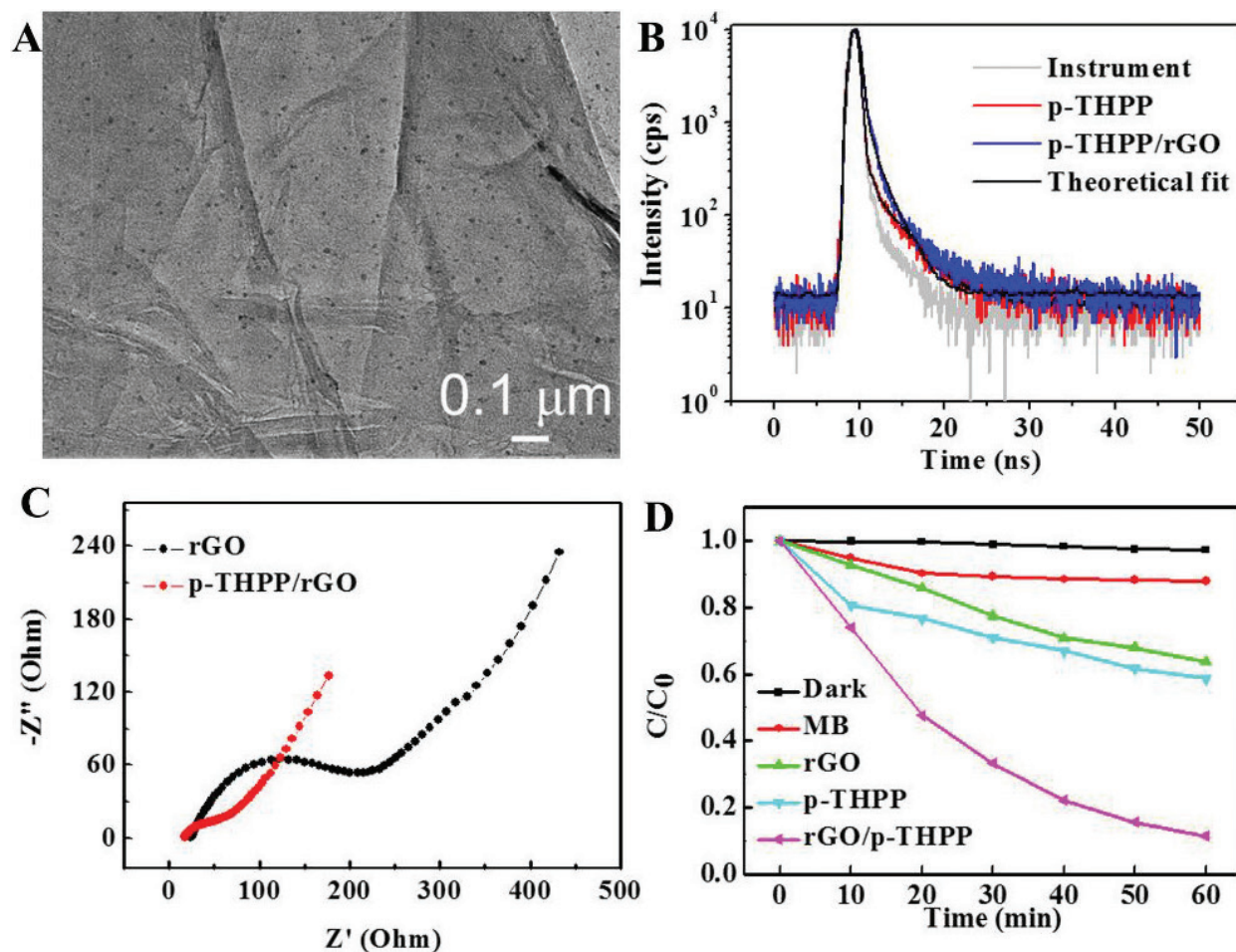


**Figure 7.** (A) TEM image of H<sub>2</sub>THPP/rGO nanohybrids; (B) the FL decay profiles of H<sub>2</sub>THPP and H<sub>2</sub>THPP/rGO nanohybrids in H<sub>2</sub>O ( $\lambda_{\text{ex}} = 405 \text{ nm}$ ); (C) Nyquist plots collected by electrical impedance spectroscopy (EIS) of free-standing rGO and H<sub>2</sub>THPP/rGO films; (D) photocatalytic degradation of MB with different samples under visible light irradiation ( $\lambda_{\text{irradiation}} > 400 \text{ nm}$ ). Adapted from Ref. [135].

## 5. Porphyrin-based PEC water splitting devices

PEC water splitting is attractive because of its ease with which an electric field can be created at the semiconductor/liquid junction to manipulate the charge transfer reaction. In water splitting, oxidation of water into O<sub>2</sub> occurs at the photoanode, and H<sup>+</sup> is reduced to H<sub>2</sub> at the photocathode. Ideally, a single semiconductor must absorb light with photon energies larger than 1.23 eV, and have a conduction band energy ( $E_{\text{cb}}$ ) and valence band energy ( $E_{\text{vb}}$ ) that straddle the electrochemical potentials  $E^\circ(\text{H}^+/\text{H}_2)$  and  $E^\circ(\text{O}_2/\text{H}_2\text{O})$ , so as to drive water splitting under illumination. Porphyrins with a band energy gap of 1.5–3.1 eV and the matched HOMO and LUMO positions are in principle able to perform this PEC reaction. As p-type semiconductors, porphyrins are usually coupled with n-type conductors to effectively motivate the water-splitting reaction. This part focuses on thin-film photoelectrodes based on porphyrin-containing systems for PEC applications.

## 5.1. Film deposition

Currently, the search of cheap and fast processing of large-area photoelectrodes is of intense research. In view of the low melting point, solubility, and flexibility, organic materials have the advantages of low-cost fabrication, and making flexible and lightweight devices. Generally, thin-film organic devices are fabricated either by vapor deposition or solution processing.

### 5.1.1. Solution-processed deposition

The solubility of organic semiconductors is a desirable characteristic in making low-cost electronic devices. As one of them, porphyrins are or can be derivatized to soluble. Therefore, thin-film porphyrins can be fabricated by solution processing near room temperature, mainly including dip coating, spin coating, or printing techniques [138, 139]. Printing methods, such as screen printing and ink jet printing, also enable fabrication and patterning of the active materials in a single step, and now the most use of them is made in fabricating organic field-effect transistors (OFETs), and organic light-emitting diodes (OLEDs) [138, 139].

Dip coating and spin coating are the most widely used methods when it comes to small-scale processing, because it is easy to handle and fairly cheap to acquire the film. In a dip-coating process, a substrate is immersed into the solution of the active materials and then exposed until dried. For instance, multilayered rGO-porphyrin films have been fabricated by alternately dipping the substrate into a GO suspension and porphyrin solutions, followed by exposure to a hydrazine vapor [96]. The resulting film showed promising applications in PEC cells.

Spin coating is often used to deposit uniform thin films to a flat substrate, simply by spreading the solution of the active material over the substrate at a high rotating speed, but this process is not quite applicable to large area, and too much material is wasted. In an example, a mixture of zinc *meso*-tetra(4-carboxyphenyl)porphyrin (ZnTCPP) and fullerene (C<sub>60</sub>) was spin-coated onto the working electrodes, and exhibited efficient photocurrent generation (IPCE value up to 47 ± 5%) [140].

### 5.1.2. Thermal vapor deposition

Vapor deposition generally includes vacuum thermal evaporation and organic vapor phase deposition (OVPD). For organic molecules that have a poor solubility, vacuum thermal evaporation is an ideal deposition method and is more suitable for multilayered fabrication or cofabrication. In a number of examples, vacuum deposition is involved to manufacture organic materials. Typically, source materials are heated under a vacuum environment, and the deposited film is usually in high uniformity. For instance, organic bilayers made of p-type porphyrin analogies (phthalocyanine) and n-type C<sub>60</sub> or PBIs have been extensively deposited by this method for PEC water splitting [141, 142]. Estimation of the film thickness and the refractive index is often conducted by ellipsometry.

An alternative to vacuum deposition is organic vapor phase deposition (OVPD). It is characterized by a process in which heating of the source materials under a stream of hot inert

gas. Then the sublimated molecules are transported to a low-temperature zone by gas flow, where molecules condensed into nanocrystals. The OVPD method offers good control over deposition efficiency and film morphology by adjusting the amount of the source materials, gas flow rate, or the collecting substrate. In our work, photocatalytic  $\text{H}_2\text{TPP}/\text{CH-PTCDI}$  junctions were codeposited via the OVPD method [126]. The two source materials were located into the upstream area with certain spacing distance because of their different sublimation temperature, and silicon wafers were put at the downstream cooled zone to collect samples with nitrogen as the carrier gas.

## 5.2. Hard porphyrin photoanodes

Appropriate choice of deposition methods makes it possible to assemble molecular, nanostructured, or thin-film porphyrins onto different electrodes. Metal substrates, such as Au, Al, or Pt, have always been involved to assemble the monolayer of porphyrin-based molecules by dip coating [143–145]. These monolayers ranged from single porphyrins to porphyrin- $\text{C}_{60}$  dyads, or ferrocene-porphyrin- $\text{C}_{60}$  triads, with an aim to increase intermolecular electron transfer. Furthermore, well-organized molecular assemblies can be achieved by covalent attachment of functional molecules to the chemically modified metals, as in the case of porphyrin alkane-thiolate with short alkanethiols on the gold nanoclusters [146], which resulted in an increased photocurrent density.

Due to the band match, other hard substrates such as ITO or FTO glasses, nanostructured  $\text{TiO}_2$ ,  $\text{SnO}_2$ , or ZnO have been employed to couple with porphyrin nanoassemblies. Of them, ITO glass is the mostly used semiconducting substrate, and a number of photoactive organic materials have been deposited on it either by spin coating or vapor deposition. As described above, different combinations of organic bilayers made of porphyrin analogies and n-type semiconductors have been fabricated on ITO by vapor deposition. For instance, organic p/n bilayer of  $\text{C}_{60}$  and 29H, 31H-phthalocyanine ( $\text{H}_2\text{Pc}$ ) was prepared by vapor deposition, and ITO glass was used as the collecting electrode [142]. As shown in **Figure 8A**, the photoanode comprised  $\text{H}_2\text{Pc}$  layer coated on ITO, and  $\text{C}_{60}$  coated on top of the  $\text{H}_2\text{Pc}$  layer (denoted as ITO/ $\text{H}_2\text{Pc}/\text{C}_{60}$ ). PEC splitting of water into  $\text{H}_2$  was confirmed across the entire visible light energy region ( $\lambda < 750$  nm) in **Figure 8B**, with the faradaic efficiency for the  $\text{H}_2$  evolution around 90%. In another work, whiskered PBIs/ $\text{H}_2\text{Pc}$  bilayer was fabricated on ITO as photoanodes (ITO/PBIs/ $\text{H}_2\text{Pc}$ ) [147]. Formation of the whiskered  $\text{H}_2\text{Pc}$  by proper thermal control resulted in an enhancement of the p/n interface. Therefore, the magnitude of the oxidation kinetics at the whiskered  $\text{H}_2\text{Pc}/\text{water}$  interface was demonstrated to be 2.5 times higher than the flat interface. We have adopted the dip-coating method to coat  $\text{H}_2\text{TPP}$  nanoparticles onto  $\text{TiO}_2$  nanotube arrays as photoanodes, leading to enhanced photocurrent generation [134]. In another study,  $\text{C}_{60}$ -ZnTPyP nanorods have been deposited onto nanostructured  $\text{SnO}_2$  films, and exhibited a power conversion efficiency of 0.63% and an IPCE of 35% [148].

## 5.3. Flexible porphyrin photoanodes

The low-temperature processing and low cost make organic devices one of the most important semiconductor devices for flexible optoelectronic device applications. Therefore, growing

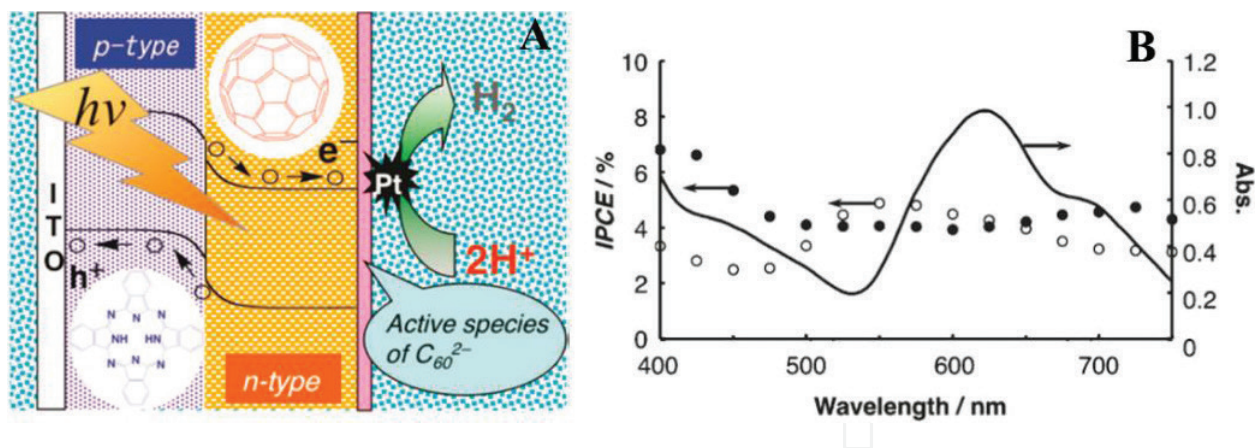


**Figure 8.** (A) An illustration of the ITO/H<sub>2</sub>Pc/C<sub>60</sub> photoanode; (B) action spectra of the photocurrent generated at ITO/H<sub>2</sub>Pc/C<sub>60</sub>-Pt (irradiation direction: ITO side (●) and Pt-coated C<sub>60</sub> side (○)) and absorption spectrum of employed bilayer (-). Adapted from Ref. [142].

development has been made on flexible organic devices, including organic solar cells, OLEDs, OFETs, sensors, and memories. As in one case of pentacene-based OFETs, 125- $\mu$ m-thick polyethylene naphthalate (PEN) film was used as a flexible substrate and 30-nm-thick pentacene was thermally deposited to create the organic active layer [149]. One early study was dealing with fully flexible OLEDs [150]. The device was built on a poly(ethylene terephthalate) substrate, with soluble polyaniline as the hole-injecting electrode, substituted poly(1,4-phenylene-vinylene) as the electroluminescent layer. Moreover, a first example of all-organic flexible photoanodes was presented to remove a gaseous pollutant (trimethylamine, TMA) [141]. Instead of ITO, H<sub>2</sub>Pc (50 nm)/PBIs (50 nm) bilayer was coated on a self-standing fluorocarbon polymer (Nafion 112) to act as a photoanode. This all-organic catalyst is responsive to full-spectrum visible light (<780 nm), which holds promise in future use inside buildings when only interior light is present.

## 6. Conclusion and perspective

To sum up, this chapter presents the recent advances on the porphyrin-based organophotocatalysts. Porphyrins possess many light conversion functionalities such as light harvesting and energy/electron transfer, and are thus acknowledged to be a promising tool in homogeneous, heterogeneous photocatalysis, or even PEC solar cells. Molecular porphyrins have easy access to other reactive species and thus render a high photocatalytic efficiency, but their limitations arise from the stability and reuse. Inclusion of porphyrin molecules onto solid supports provides a robust material that can be easily recovered for successive use. In the series of solid supports, the electron-accepting and electron-conducting carbon materials are preferred in initiating an increased PET mechanism. Their large surface area also allows for high-loading content. Nanoassembly makes heterogenization of porphyrins a further step forward, opening a way to control the light conversion functionality in the aggregated state. Ordered molecular alignment is attainable by proper control over the supramolecular assembly, thus resulting in enhanced light-harvesting and charge-transfer efficiencies. Promoted

charge transfer can also be fulfilled by a combination of nanostructured porphyrins with other acceptor materials, such as metals, inorganic semiconductors, and organic electron acceptors. Moreover, porphyrins can be fabricated onto hard or flexible/stretchable electrodes by low-temperature solution processing or vapor deposition, which finds wide applications in PEC solar cells.

Despite the current knowledge of the organic/inorganic hybrid, an in-depth insight into the interface geometry is essential in determining and understanding the properties and functions of the two different material classes. Supplementary information can be provided by rational calculation and simulation, especially in light of the electronic properties, excitation dynamics, and charge transport of the hybrid materials. Further efforts are required to align these molecular assemblies onto any desired substrate at the macroscopic level. The resulting collective effect will finally lead to remarkable improvement on light conversion efficiency for practical applications in optoelectronic devices.

## Acknowledgements

Authors are grateful for the National Natural Science Foundation of China (Grant nos. 51503014 and 51501008).

## Author details

Yingzhi Chen<sup>1</sup>, Zheng-Hong Huang<sup>2\*</sup> and Lu-Ning Wang<sup>1</sup>

\*Address all correspondence to: zhhuang@mail.tsinghua.edu.cn

1 School of Materials Science and Engineering, University of Science and Technology Beijing, Beijing, China

2 Key Laboratory of Advanced Materials (MOE), School of Materials Science and Engineering, Tsinghua University, Beijing, China

## References

- [1] Chen C, Ma W, Zhao J. Semiconductor-mediated photodegradation of pollutants under visible-light irradiation. *Chemical Society Reviews*. 2010;**39**:4206-4219. DOI: 10.1039/b921692h
- [2] Maeda K, Domen K. Photocatalytic water splitting: Recent progress and future challenges. *The Journal of Physical Chemistry Letters*. 2010;**1**:2655-2661. DOI: 10.1021/jz1007966
- [3] Maeda K, Teramura K, Lu D, Takata T, Saito N, Inoue Y, et al. Photocatalyst releasing hydrogen from water. *Nature*. 2006;**440**:295. DOI: 10.1038/440295a

- [4] Esswein AJ, Nocera DG. Hydrogen production by molecular photocatalysis. *Chemical Reviews*. 2007;**107**:4022-4047. DOI: 10.1021/cr050193e
- [5] Chen X, Shen S, Guo L, Mao SS. Semiconductor-based photocatalytic hydrogen generation. *Chemical Reviews*. 2010;**110**:6503-6570. DOI: 10.1021/cr1001645
- [6] Wang X, Liow C, Bisht A, Liu X, Sum TC, Chen X, et al. Engineering interfacial photo-induced charge transfer based on nanobamboo array architecture for efficient solar-to-chemical energy conversion. *Advanced Materials*. 2015;**27**:2207-2214. DOI: 10.1002/adma.201405674
- [7] Wang X, Liow C, Qi D, Zhu B, Leow WR, Wang H, et al. Programmable photo-electrochemical hydrogen evolution based on multi-segmented CdS-Au nanorod arrays. *Advanced Materials*. 2014;**26**:3506-3512. DOI: 10.1002/adma.201306201
- [8] Chen Y, Li A, Yue X, Wang L-N, Huang Z-H, Kang F, et al. Facile fabrication of organic/inorganic nanotube heterojunction arrays for enhanced photoelectrochemical water splitting. *Nanoscale*. 2016;**8**:13228-13235. DOI: 10.1039/c5nr07893h
- [9] Schneider J, Matsuoka M, Takeuchi M, Zhang J, Horiuchi Y, Anpo M, et al. Understanding TiO<sub>2</sub> photocatalysis: Mechanisms and materials. *Chemical Reviews*. 2014;**114**:9919-9986. DOI: 10.1021/cr5001892
- [10] Lu D, Fang P, Wu W, Ding J, Jiang L, Zhao X, et al. Solvothermal-assisted synthesis for self-assembling TiO<sub>2</sub> nanorods on large graphitic carbon nitride sheets with their anti-recombination in photocatalytic removal of Cr (VI) and rhodamin B under visible light irradiation. *Nanoscale*. 2017;**9**:3231-3245. DOI: 10.1039/C6NR09137G
- [11] Cushing SK, Meng F, Zhang J, Ding B, Chen CK, Chen C-J, et al. Effects of defects on photocatalytic activity of hydrogen-treated titanium oxide nanobelts. *ACS Catalysis*. 2017;**7**:1742-1748. DOI: 10.1021/acscatal.6b02177
- [12] Wang J, Waters JL, Kung P, Kim SM, Kelly JT, McNamara LE, et al. A facile electrochemical reduction method for improving photocatalytic performance of  $\alpha$ -Fe<sub>2</sub>O<sub>3</sub> photoanode for solar water splitting. *ACS Applied Materials & Interfaces*. 2017;**9**:381-390. DOI: 10.1021/acsami.6b11057
- [13] Bhoi Y, Mishra B. Single step combustion synthesis, characterization and photocatalytic application of  $\alpha$ -Fe<sub>2</sub>O<sub>3</sub>-Bi<sub>2</sub>S<sub>3</sub> heterojunctions for efficient and selective reduction of structurally diverse nitroarenes. *Chemical Engineering Journal*. 2017;**316**:70-81. DOI: 10.1016/j.cej.2017.01.075
- [14] Yang J, Wu Q, Yang X, He S, Khan J, Meng Y, et al. Chestnut-like TiO<sub>2</sub>@  $\alpha$ -Fe<sub>2</sub>O<sub>3</sub> core-shell nanostructures with abundant interfaces for efficient and ultralong life lithium ion storage. *ACS Applied Materials & Interfaces*. 2017;**9**:354-361. DOI: 10.1021/acsami.6b12150
- [15] Barhoum A, Melcher J, Van Assche G, Rahier H, Bechelany M, Fleisch M, et al. Synthesis, growth mechanism, and photocatalytic activity of zinc oxide nanostructures: Porous microparticles versus nonporous nanoparticles. *Journal of Materials Science*. 2017;**52**:2746-2762. DOI: 10.1007/s10853-016-0567-3

- [16] Gupta R, Eswar NK, Modak JM, Madras G. Effect of morphology of zinc oxide in ZnO-CdS-Ag ternary nanocomposite towards photocatalytic inactivation of *E. coli* under UV and visible light. *Chemical Engineering Journal*. 2017;**307**:966-980. DOI: 10.1016/j.cej.2016.08.142
- [17] Wu SC, Tan CS, Huang MH. Strong facet effects on interfacial charge transfer revealed through the examination of photocatalytic activities of various Cu<sub>2</sub>O-ZnO heterostructures. *Advanced Functional Materials*. 2017;**27**:1604635. DOI: 10.1002/adfm.201604635
- [18] Zhang Y, Zhou X, Zhao Y, Liu Z, Ma D, Chen S, et al. One-step solvothermal synthesis of interlaced nanoflake-assembled flower-like hierarchical Ag/Cu<sub>2</sub>O composite microspheres with enhanced visible light photocatalytic properties. *RSC Advances*. 2017;**7**:6957-6965. DOI: 10.1039/C6RA26870F
- [19] Lou Z, Li Y, Zhu L, Niu W, Song H, Ye Z, et al. The crystalline/amorphous contact in Cu<sub>2</sub>O/Ta<sub>2</sub>O<sub>5</sub> heterostructures: Increasing its sunlight-driven overall water splitting efficiency. *Journal of Materials Chemistry A*. 2017;**5**:2732-2738. DOI: 10.1039/C6TA10728A
- [20] Samsudin EM, Hamid SBA. Effect of band gap engineering in anionic-doped TiO<sub>2</sub> photocatalyst. *Applied Surface Science*. 2017;**391**:326-336. DOI: 10.1016/j.apsusc.2016.07.007
- [21] Chen J, Wu G, Wang T, Li X, Li M, Sang Y, et al. Carrier step-by-step transport initiated by precise defect distribution engineering for efficient photocatalytic hydrogen generation. *ACS Applied Materials & Interfaces*. 2017;**9**:4634-4642. DOI: 10.1021/acsami.6b14700
- [22] Low J, Cheng B, Yu J. Surface modification and enhanced photocatalytic CO<sub>2</sub> reduction performance of TiO<sub>2</sub>: A review. *Applied Surface Science*. 2017;**392**:658-686. DOI: 10.1016/j.apsusc.2016.09.093
- [23] Jin Z, Liu C, Qi K, Cui X. Photo-reduced Cu/CuO nanoclusters on TiO<sub>2</sub> nanotube arrays as highly efficient and reusable catalyst. *Scientific Reports*. 2017;**7**:39695. DOI:10.1038/srep39695
- [24] Wang T, Lv R, Zhang P, Li C, Gong J. Au nanoparticle sensitized ZnO nanopencil arrays for photoelectrochemical water splitting. *Nanoscale*. 2015;**7**:77-81. DOI: 10.1039/C4NR03735A
- [25] Forrest SR, Thompson ME. Introduction: Organic electronics and optoelectronics. *Chemical Reviews*. 2007;**107**:923-925. DOI: 10.1021/cr0501590
- [26] Zhao YS, Fu H, Peng A, Ma Y, Liao Q, Yao J. Construction and optoelectronic properties of organic one-dimensional nanostructures. *Accounts of Chemical Research*. 2009;**43**:409-418. DOI: 10.1021/ar900219n
- [27] Kelley TW, Baude PF, Gerlach C, Ender DE, Muyres D, Haase MA, et al. Recent progress in organic electronics: Materials, devices, and processes. *Chemistry of Materials*. 2004;**16**:4413-4422. DOI: 10.1021/cm049614j
- [28] Zhao YS, Fu H, Peng A, Ma Y, Xiao D, Yao J. Low-dimensional nanomaterials based on small organic molecules: Preparation and optoelectronic properties. *Advanced Materials*. 2008;**20**:2859-2876. DOI: 10.1002/adma.200800604

- [29] Zang L, Che Y, Moore JS. One-dimensional self-assembly of planar  $\pi$ -conjugated molecules: Adaptable building blocks for organic nanodevices. *Accounts of Chemical Research*. 2008;**41**:1596-1608. DOI: 10.1021/ar800030w
- [30] Li Y, Wang W, Leow WR, Zhu B, Meng F, Zheng L, et al. Optoelectronics of organic nanofibers formed by co-assembly of porphyrin and perylenediimide. *Small*. 2014;**10**:2776-2781. DOI: 10.1002/sml.201302964
- [31] Chen Y, Li A, Huang Z-H, Wang L-N, Kang F. Porphyrin-based nanostructures for photocatalytic applications. *Nanomaterials*. 2016;**6**:51. DOI:10.3390/nano6030051
- [32] Hasobe T. Porphyrin-based supramolecular nanoarchitectures for solar energy conversion. *The Journal of Physical Chemistry Letters*. 2013;**4**:1771-1780. DOI: 10.1021/jz4005152
- [33] Medforth CJ, Wang Z, Martin KE, Song Y, Jacobsen JL, Shelnutt JA. Self-assembled porphyrin nanostructures. *Chemical Communications*. 2009;**35**:7261-7277. DOI: 10.1039/B914432C
- [34] Hasobe T, Imahori H, Kamat PV, Fukuzumi S. Quaternary self-organization of porphyrin and fullerene units by clusterization with gold nanoparticles on SnO<sub>2</sub> electrodes for organic solar cells. *Journal of the American Chemical Society*. 2003;**125**:14962-14963. DOI: 10.1021/ja0377192
- [35] Hasobe T, Saito K, Kamat PV, Troiani V, Qiu H, Solladié N, et al. Organic solar cells. Supramolecular composites of porphyrins and fullerenes organized by polypeptide structures as light harvesters. *Journal of Materials Chemistry*. 2007;**17**:4160-4170. DOI: 10.1039/B706678C
- [36] Noh YY, Kim JJ, Yoshida Y, Yase K. Effect of molecular orientation of epitaxially grown platinum (II) octaethyl porphyrin films on the performance of field-effect transistors. *Advanced Materials*. 2003;**15**:699-702. DOI: 10.1002/adma.200304005
- [37] Che CM, Xiang HF, Chui SSY, Xu ZX, Roy VeAeL, Yan JJ, et al. A high-performance organic field-effect transistor based on platinum (II) porphyrin: Peripheral substituents on porphyrin ligand significantly affect film structure and charge mobility. *Chemistry, an Asian Journal*. 2008;**3**:1092-1103. DOI: 10.1002/asia.200800011
- [38] Endo A, Ogasawara M, Takahashi A, Yokoyama D, Kato Y, Adachi C. Thermally activated delayed fluorescence from Sn<sup>4+</sup>-porphyrin complexes and their application to organic light emitting diodes—A novel mechanism for electroluminescence. *Advanced Materials*. 2009;**21**:4802-4806. DOI: 10.1002/adma.200900983
- [39] Li B, Li J, Fu Y, Bo Z. Porphyrins with four monodisperse oligofluorene arms as efficient red light-emitting materials. *Journal of the American Chemical Society*. 2004;**126**:3430-3431. DOI: 10.1021/ja039832y
- [40] Marin ML, Santos-Juanes L, Arques A, Amat AM, Miranda MA. Organic photocatalysts for the oxidation of pollutants and model compounds. *Chemical Reviews*. 2011;**112**:1710-1750. DOI: 10.1021/cr2000543

- [41] Kim W, Park J, Jo HJ, Kim H-J, Choi W. Visible light photocatalysts based on homogeneous and heterogenized tin porphyrins. *The Journal of Physical Chemistry C*. 2008;**112**:491-499. DOI: 10.1021/jp0747151
- [42] Craw M, Redmond R, Truscott TG. Laser flash photolysis of haematoporphyrins in some homogeneous and heterogeneous environments. *Journal of the Chemical Society, Faraday Transactions 1: Physical Chemistry in Condensed Phases*. 1984;**80**:2293-2299. DOI: 10.1039/F19848002293
- [43] Imahori H, Ueda M, Kang S, Hayashi H, Hayashi S, Kaji H, et al. Effects of porphyrin substituents on film structure and photoelectrochemical properties of porphyrin/fullerene composite clusters electrophoretically deposited on nanostructured SnO<sub>2</sub> electrodes. *Chemistry–A European Journal*. 2007;**13**:10182-10193. DOI: 10.1002/chem.200700446
- [44] Umeyama T, Mihara J, Tezuka N, Matano Y, Stranius K, Chukharev V, et al. Preparation and photophysical and photoelectrochemical properties of a covalently fixed porphyrin–chemically converted graphene composite. *Chemistry–A European Journal*. 2012;**18**:4250-4257. DOI: 10.1002/chem.201103843
- [45] Kay A, Graetzel M. Artificial photosynthesis. 1. Photosensitization of titania solar cells with chlorophyll derivatives and related natural porphyrins. *The Journal of Physical Chemistry*. 1993;**97**:6272-6277
- [46] Nazeeruddin MK, Humphry-Baker R, Officer DL, Campbell WM, Burrell AK, Grätzel M. Application of metalloporphyrins in nanocrystalline dye-sensitized solar cells for conversion of sunlight into electricity. *Langmuir*. 2004;**20**:6514-6517. DOI: 10.1021/la0496082
- [47] Hori T, Aratani N, Takagi A, Matsumoto T, Kawai T, Yoon MC, et al. Giant porphyrin wheels with large electronic coupling as models of light-harvesting photosynthetic antenna. *Chemistry–A European Journal*. 2006;**12**:1319-1327. DOI: 10.1002/chem.200501373
- [48] Imahori H, Umeyama T, Ito S. Large  $\pi$ -aromatic molecules as potential sensitizers for highly efficient dye-sensitized solar cells. *Accounts of Chemical Research*. 2009;**42**:1809-1818. DOI: 10.1021/ar900034t
- [49] Mathew S, Yella A, Gao P, Humphry-Baker R, Curchod BF, Ashari-Astani N, et al. Dye-sensitized solar cells with 13% efficiency achieved through the molecular engineering of porphyrin sensitizers. *Nature Chemistry*. 2014;**6**:242-247. DOI: 10.1038/nchem.1861
- [50] Martinez-Diaz MV, de la Torre G, Torres T. Lighting porphyrins and phthalocyanines for molecular photovoltaics. *Chemical Communications*. 2010;**46**:7090-7108. DOI: 10.1039/C0CC02213F
- [51] Drobizhev M, Karotki A, Kruk M, Mamardashvili NZ, Rebane A. Drastic enhancement of two-photon absorption in porphyrins associated with symmetrical electron-accepting substitution. *Chemical Physics Letters*. 2002;**361**:504-512. DOI: 10.1016/S0009-2614(02)00999-5

- [52] Suslick KS, Rakow NA, Kosal ME, Chou J-H. The materials chemistry of porphyrins and metalloporphyrins. *Journal of Porphyrins and Phthalocyanines*. 2000;**4**:407-413. DOI: 10.1002/(SICI)1099-1409(200006/07)4:4<407::AID-JPP256>3.0.CO;2-5
- [53] Gao W-Y, Chrzanowski M, Ma S. Metal-metalloporphyrin frameworks: A resurging class of functional materials. *Chemical Society Reviews*. 2014;**43**:5841-5866. DOI: 10.1039/C4CS00001C
- [54] Zheng W, Shan N, Yu L, Wang X. UV-visible, fluorescence and EPR properties of porphyrins and metalloporphyrins. *Dyes and Pigments*. 2008;**77**:153-157. DOI: 10.1016/j.dyepig.2007.04.007
- [55] Shiragami T, Matsumoto J, Inoue H, Yasuda M. Antimony porphyrin complexes as visible-light driven photocatalyst. *Journal of Photochemistry and Photobiology C*. 2005;**6**:227-248. DOI: 10.1016/j.jphotochemrev.2005.12.001
- [56] Gao P, Konrad D, Aghazada S, Nazeeruddin MK. Molecular engineering of functional materials for energy and opto-electronic applications. *CHIMIA International Journal for Chemistry*. 2015;**69**:253-263
- [57] Xue X, Zhang W, Zhang N, Ju C, Peng X, Yang Y, et al. Effect of the length of the alkyl chains in porphyrin meso-substituents on the performance of dye-sensitized solar cells. *RSC Advances*. 2014;**4**:8894-8900. DOI: 10.1039/C3RA46212A
- [58] Ladomenou K, Kitsopoulos T, Sharma G, Coutsolelos A. The importance of various anchoring groups attached on porphyrins as potential dyes for DSSC applications. *RSC Advances*. 2014;**4**:21379-21404. DOI: 10.1039/C4RA00985A
- [59] Liu B, Zhu W, Wang Y, Wu W, Li X, Chen B, et al. Modulation of energy levels by donor groups: An effective approach for optimizing the efficiency of zinc-porphyrin based solar cells. *Journal of Materials Chemistry*. 2012;**22**:7434-7444. DOI: 10.1039/C2JM16804A
- [60] Monteiro CJ, Pereira MM, Azenha ME, Burrows HD, Serpa C, Arnaut LG, et al. A comparative study of water soluble 5, 10, 15, 20-tetrakis (2, 6-dichloro-3-sulfophenyl) porphyrin and its metal complexes as efficient sensitizers for photodegradation of phenols. *Photochemical & Photobiological Sciences*. 2005;**4**:617-624. DOI: 10.1039/B507597A
- [61] Maldotti A, Molinari A, Andreotti L, Fogagnolo M, Amadelli R. Novel reactivity of photoexcited iron porphyrins caged into a polyfluoro sulfonated membrane in catalytic hydrocarbon oxygenation. *Chemical Communications*. 1998;**24**:507-508. DOI: 10.1039/A706237K.
- [62] Tomé JP, Neves MG, Tomé AC, Cavaleiro JA, Soncin M, Magaraggia M, et al. Synthesis and antibacterial activity of new poly-s-lysine-porphyrin conjugates. *Journal of Medicinal Chemistry*. 2004;**47**:6649-6652. DOI: 10.1021/jm040802v
- [63] Caminos DA, Spesia MB, Durantini EN. Photodynamic inactivation of escherichia coli by novel meso-substituted porphyrins by 4-(3-N,N,N-trimethylammoniumpropoxy) phenyl and 4-(trifluoromethyl) phenyl groups. *Photochemical & Photobiological Sciences*. 2006;**5**:56-65. DOI: 10.1039/B513511G

- [64] Carvalho CM, Tome JP, Faustino MA, Neves MG, Tome AC, Cavaleiro JA, et al. Antimicrobial photodynamic activity of porphyrin derivatives: Potential application on medical and water disinfection. *Journal of Porphyrins and Phthalocyanines*. 2009;**13**:574-577. DOI: 10.1142/S1088424609000528
- [65] Murtinho D, Pineiro M, Pereira MM, Gonsalves AMdAR, Arnaut LG, da Graça Miguel M, et al. Novel porphyrins and a chlorin as efficient singlet oxygen photosensitizers for photooxidation of naphthols or phenols to quinones. *Journal of the Chemical Society, Perkin Transactions 2*. 2000;**12**:2441-2447. DOI: 10.1039/B006583H
- [66] Ribeiro SM, Serra AC, Gonsalves AdAR. Covalently immobilized porphyrins on silica modified structures as photooxidation catalysts. *Journal of Molecular Catalysis A: Chemical*. 2010;**326**:121-127. DOI: 10.1016/j.molcata.2010.05.001
- [67] Cai J-H, Huang J-W, Yu H-C, Ji L-N. Fabrication and characterizations of silica composite microspheres immobilized with porphyrins and their photocatalytic properties. *Journal of the Taiwan Institute of Chemical Engineers*. 2012;**43**:958-964. DOI: 10.1016/j.jtice.2012.05.004
- [68] Silva E, Pereira MM, Burrows HD, Azenha M, Sarakha M, Bolte M. Photooxidation of 4-chlorophenol sensitised by iron meso-tetrakis (2,6-dichloro-3-sulfophenyl) porphyrin in aqueous solution. *Photochemical & Photobiological Sciences*. 2004;**3**:200-204. DOI: 10.1039/B308975D
- [69] Rebelo SL, Melo A, Coimbra R, Azenha ME, Pereira MM, Burrows HD, et al. Photodegradation of atrazine and ametryn with visible light using water soluble porphyrins as sensitizers. *Environmental Chemistry Letters*. 2007;**5**:29-33. DOI: 10.1007/s10311-006-0072-z
- [70] Harmon HJ. Photocatalytic demethylation of 2,4,6-trinitrotoluene (TNT) by porphyrins. *Chemosphere*. 2006;**63**:1094-1097. DOI: 10.1016/j.chemosphere.2005.09.013
- [71] Qian D-J, Wenk S-O, Nakamura C, Wakayama T, Zorin N, Miyake J. Photoinduced hydrogen evolution by use of porphyrin, EDTA, viologens and hydrogenase in solutions and Langmuir-Blodgett films. *International Journal of Hydrogen Energy*. 2002;**27**:1481-1487. DOI: 10.1016/S0360-3199(02)00104-0
- [72] Lazarides T, Delor M, Sazanovich IV, McCormick TM, Georgakaki I, Charalambidis G, et al. Photocatalytic hydrogen production from a noble metal free system based on a water soluble porphyrin derivative and a cobaloxime catalyst. *Chemical Communications*. 2014;**50**:521-523. DOI: 10.1039/C3CC45025B
- [73] Nakazono T, Parent AR, Sakai K. Cobalt porphyrins as homogeneous catalysts for water oxidation. *Chemical Communications*. 2013;**49**:6325-6327. DOI: 10.1039/C3CC43031F
- [74] Natali M, Luisa A, Iengo E, Scandola F. Efficient photocatalytic hydrogen generation from water by a cationic cobalt (II) porphyrin. *Chemical Communications*. 2014;**50**:1842-1844. DOI: 10.1039/C3CC48882A

- [75] Cai J-H, Huang J-W, Zhao P, Ye Y-J, Yu H-C, Ji L-N. Silica microspheres functionalized with porphyrin as a reusable and efficient catalyst for the photooxidation of 1, 5-dihydroxynaphthalene in aerated aqueous solution. *Journal of Photochemistry and Photobiology A: Chemistry*. 2009;**207**:236-243. DOI: 10.1016/j.jphotochem.2009.07.016
- [76] Bedioui F. Zeolite-encapsulated and clay-intercalated metal porphyrin, phthalocyanine and Schiff-base complexes as models for biomimetic oxidation catalysts: An overview. *Coordination Chemistry Reviews*. 1995;**144**:39-68. DOI: 10.1016/0010-8545(94)08000-H
- [77] Skrobot F, Valente A, Neves G, Rosa I, Rocha J, Cavaleiro J. Monoterpenes oxidation in the presence of Y zeolite-entrapped manganese (III) tetra (4-N-benzylpyridyl) porphyrin. *Journal of Molecular Catalysis A: Chemical*. 2003;**201**:211-222. DOI: 10.1016/S1381-1169(03)00181-X
- [78] Johnson Inbaraj J, Vinodu MV, Gandhidasan R, Murugesan R, Padmanabhan M. Photosensitizing properties of ionic porphyrins immobilized on functionalized solid polystyrene support. *Journal of Applied Polymer Science*. 2003;**89**:3925-3930. DOI: 10.1002/app.12610
- [79] Yuan H, Wang B, Lv F, Liu L, Wang S. Conjugated-polymer-based energy-transfer systems for antimicrobial and anticancer applications. *Advanced Materials*. 2014;**26**:6978-6982. DOI: 10.1002/adma.201400379
- [80] Huang G, Guo C-C, Tang S-S. Catalysis of cyclohexane oxidation with air using various chitosan-supported metallotetraphenylporphyrin complexes. *Journal of Molecular Catalysis A: Chemical*. 2007;**261**:125-130. DOI: 10.1016/j.molcata.2006.08.014
- [81] Bozja J, Sherrill J, Michielsen S, Stojiljkovic I. Porphyrin-based, light-activated antimicrobial materials. *Journal of Polymer Science Part A: Polymer Chemistry*. 2003;**41**:2297-2303. DOI: 10.1002/pola.10773
- [82] Pepe E, Abbas O, Rebufa C, Simon M, Lacombe S, Julliard M. Supported photosensitizers for the visible light activation of phenols towards oxygen. *Journal of Photochemistry and Photobiology A: Chemistry*. 2005;**170**:143-149. DOI: 10.1016/j.jphotochem.2004.06.019
- [83] Hequet V, Le Cloirec P, Gonzalez C, Meunier B. Photocatalytic degradation of atrazine by porphyrin and phthalocyanine complexes. *Chemosphere*. 2000;**41**:379-386. DOI: 10.1016/S0045-6535(99)00474-9
- [84] Tkachenko NV, Lemmetyinen H, Sonoda J, Ohkubo K, Sato T, Imahori H, et al. Ultrafast photodynamics of exciplex formation and photoinduced electron transfer in porphyrin-fullerene dyads linked at close proximity. *The Journal of Physical Chemistry A*. 2003;**107**:8834-8844. DOI: 10.1021/jp035412j
- [85] Tsue H, Imahori H, Kaneda T, Tanaka Y, Okada T, Tamaki K, et al. Large acceleration effect of photoinduced electron transfer in porphyrin-quinone dyads with a rigid spacer involving a dihalosubstituted three-membered ring. *Journal of the American Chemical Society*. 2000;**122**:2279-2288. DOI: 10.1021/ja9900454

- [86] Baskaran D, Mays JW, Zhang XP, Bratcher MS. Carbon nanotubes with covalently linked porphyrin antennae: Photoinduced electron transfer. *Journal of the American Chemical Society*. 2005;**127**:6916-6917. DOI: 10.1021/ja0508222
- [87] Zhu M, Li Z, Xiao B, Lu Y, Du Y, Yang P, et al. Surfactant assistance in improvement of photocatalytic hydrogen production with the porphyrin noncovalently functionalized graphene nanocomposite. *ACS Applied Materials & Interfaces*. 2013;**5**:1732-1740. DOI: 10.1021/am302912v
- [88] Chen D, Wang K, Hong W, Zong R, Yao W, Zhu Y. Visible light photoactivity enhancement via CuTCPP hybridized g-C<sub>3</sub>N<sub>4</sub> nanocomposite. *Applied Catalysis B: Environmental*. 2015;**166**:366-373. DOI: 10.1016/j.apcatb.2014.11.050
- [89] Baba A, Matsuzawa T, Sriwichai S, Ohdaira Y, Shinbo K, Kato K, et al. Enhanced photocurrent generation in nanostructured chromophore/carbon nanotube hybrid layer-by-layer multilayers. *The Journal of Physical Chemistry C*. 2010;**114**:14716-14721. DOI: 10.1021/jp103121m
- [90] Das SK, Subbaiyan NK, D'Souza F, Sandanayaka AS, Wakahara T, Ito O. Formation and photoinduced properties of zinc porphyrin-SWCNT and zinc phthalocyanine-SWCNT nanohybrids using diameter sorted nanotubes assembled via metal-ligand coordination and  $\pi$ - $\pi$  stacking. *Journal of Porphyrins and Phthalocyanines*. 2011;**15**:1033-1043. DOI: 10.1142/S1088424611003951
- [91] Banerjee I, Mondal D, Martin J, Kane RS. Photoactivated antimicrobial activity of carbon nanotube-porphyrin conjugates. *Langmuir*. 2010;**26**:17369-17374. DOI: 10.1021/la103298e
- [92] Xiang Q, Yu J, Jaroniec M. Graphene-based semiconductor photocatalysts. *Chemical Society Reviews*. 2012;**41**:782-796. DOI: 10.1039/C1CS15172J
- [93] Kamat PV. Graphene-based nanoassemblies for energy conversion. *The Journal of Physical Chemistry Letters*. 2011;**2**:242-251. DOI: 10.1021/jz101639v
- [94] Xiang Q, Yu J. Graphene-based photocatalysts for hydrogen generation. *The Journal of Physical Chemistry Letters*. 2013;**4**:753-759. DOI: 10.1021/jz302048d
- [95] Zhang Z, Zhu J, Han Q, Cui H, Bi H, Wang X. Enhanced photo-electrochemical performances of graphene-based composite functionalized by Zn<sup>2+</sup> tetraphenylporphyrin. *Applied Surface Science*. 2014;**321**:404-411. DOI: 10.1016/j.apsusc.2014.10.043
- [96] Sun J, Meng D, Jiang S, Wu G, Yan S, Geng J, et al. Multiple-bilayered RGO-porphyrin films: From preparation to application in photoelectrochemical cells. *Journal of Materials Chemistry*. 2012;**22**:18879-17886. DOI: 10.1039/C2JM33900E
- [97] Lu Q, Zhang Y, Liu S. Graphene quantum dots enhanced photocatalytic activity of zinc porphyrin toward the degradation of methylene blue under visible-light irradiation. *Journal of Materials Chemistry A*. 2015;**3**:8552-8558. DOI: 10.1039/C5TA00525F

- [98] Xu Y, Liu Z, Zhang X, Wang Y, Tian J, Huang Y, et al. A graphene hybrid material covalently functionalized with porphyrin: Synthesis and optical limiting property. *Advanced Materials*. 2009;**21**:1275-1279. DOI: 10.1002/adma.200801617
- [99] Wang H-X, Zhou K-G, Xie Y-L, Zeng J, Chai N-N, Li J, et al. Photoactive graphene sheets prepared by "click" chemistry. *Chemical Communications*. 2011;**47**:5747-5749. DOI: 10.1039/C1CC11121C
- [100] Ge R, Li X, Kang S-Z, Qin L, Li G. Highly efficient graphene oxide/porphyrin photocatalysts for hydrogen evolution and the interfacial electron transfer. *Applied Catalysis B: Environmental*. 2016;**187**:67-74. DOI: 10.1016/j.apcatb.2016.01.024
- [101] Cao S, Yu J. g-C<sub>3</sub>N<sub>4</sub>-based photocatalysts for hydrogen generation. *The Journal of Physical Chemistry Letters*. 2014;**5**:2101-2107. DOI: 10.1021/jz500546b
- [102] Wang X, Maeda K, Thomas A, Takane K, Xin G, Carlsson JM, et al. A metal-free polymeric photocatalyst for hydrogen production from water under visible light. *Nature Materials*. 2009;**8**:76-80. DOI: 10.1038/nmat2317
- [103] Zheng Y, Liu J, Liang J, Jaroniec M, Qiao SZ. Graphitic carbon nitride materials: Controllable synthesis and applications in fuel cells and photocatalysis. *Energy & Environmental Science*. 2012;**5**:6717-6731. DOI: 10.1039/C2EE03479D
- [104] Niu P, Zhang L, Liu G, Cheng HM. Graphene-like carbon nitride nanosheets for improved photocatalytic activities. *Advanced Functional Materials*. 2012;**22**:4763-4770. DOI: 10.1002/adfm.201200922
- [105] Chen X, Lu W, Xu T, Li N, Qin D, Zhu Z, et al. A bio-inspired strategy to enhance the photocatalytic performance of g-C<sub>3</sub>N<sub>4</sub> under solar irradiation by axial coordination with hemin. *Applied Catalysis B: Environmental*. 2017;**201**:518-526. DOI: 10.1016/j.apcatb.2016.08.020
- [106] Zhao G, Pang H, Liu G, Li P, Liu H, Zhang H, et al. Co-porphyrin/carbon nitride hybrids for improved photocatalytic CO<sub>2</sub> reduction under visible light. *Applied Catalysis B: Environmental*. 2017;**200**:141-149. DOI: 10.1016/j.apcatb.2016.06.074
- [107] Vasilopoulou M, Douvas AM, Georgiadou DG, Constantoudis V, Davazoglou D, Kennou S, et al. Large work function shift of organic semiconductors inducing enhanced interfacial electron transfer in organic optoelectronics enabled by porphyrin aggregated nanostructures. *Nano Research*. 2014;**7**:679-693. DOI: 10.1007/s12274-014-0428-9
- [108] Liu H, Xu J, Li Y, Li Y. Aggregate nanostructures of organic molecular materials. *Accounts of Chemical Research*. 2010;**43**:1496-1508. DOI: 10.1021/ar100084y
- [109] Lee SJ, Hupp JT, Nguyen ST. Growth of narrowly dispersed porphyrin nanowires and their hierarchical assembly into macroscopic columns. *Journal of the American Chemical Society*. 2008;**130**:9632-9633. DOI: 10.1021/ja801733t
- [110] Hu J-S, Guo Y-G, Liang H-P, Wan L-J, Jiang L. Three-dimensional self-organization of supramolecular self-assembled porphyrin hollow hexagonal nanoprisms. *Journal of the American Chemical Society*. 2005;**127**:17090-17095. DOI: 10.1021/ja0553912

- [111] Yoon SM, Hwang IC, Kim KS, Choi HC. Synthesis of single-crystal tetra (4-pyridyl) porphyrin rectangular nanotubes in the vapor phase. *Angewandte Chemie International Edition*. 2009;**48**:2506-2509. DOI: 10.1002/anie.200806301
- [112] Guo P, Chen P, Liu M. Porphyrin assemblies via a surfactant-assisted method: From nanospheres to nanofibers with tunable length. *Langmuir*. 2012;**28**:15482-15490. DOI: 10.1021/la3033594
- [113] Atula S. Sonication-assisted supramolecular nanorods of meso-diaryl-substituted porphyrins. *Chemical Communications*. 2008;**24**:724-726. DOI: 10.1039/B713971C
- [114] Wang Z, Medforth CJ, Shelnutt JA. Porphyrin nanotubes by ionic self-assembly. *Journal of the American Chemical Society*. 2004;**126**:15954-15955. DOI: 10.1021/ja045068j
- [115] Wasielewski MR. Self-assembly strategies for integrating light harvesting and charge separation in artificial photosynthetic systems. *Accounts of Chemical Research*. 2009;**42**:1910-1921. DOI: 10.1021/ar9001735
- [116] Sakuma T, Sakai H, Hasobe T. Preparation and structural control of metal coordination-assisted supramolecular architectures of porphyrins. Nanocubes to microrods. *Chemical Communications*. 2012;**48**:4441-4443. DOI: 10.1039/C2CC30756A
- [117] Motoyama S, Makiura R, Sakata O, Kitagawa H. Highly crystalline nanofilm by layering of porphyrin metal-organic framework sheets. *Journal of the American Chemical Society*. 2011;**133**:5640-5643. DOI: 10.1021/ja110720f
- [118] Guo P, Chen P, Ma W, Liu M. Morphology-dependent supramolecular photocatalytic performance of porphyrin nanoassemblies: From molecule to artificial supramolecular nanoantenna. *Journal of Materials Chemistry*. 2012;**22**:20243-20249. DOI: 10.1039/C2JM33253A
- [119] Hasobe T, Sakai H, Mase K, Ohkubo K, Fukuzumi S. Remarkable enhancement of photocatalytic hydrogen evolution efficiency utilizing an internal cavity of supramolecular porphyrin hexagonal nanocylinders under visible-light irradiation. *The Journal of Physical Chemistry C*. 2013;**117**:4441-4449. DOI: 10.1021/jp400381h
- [120] Zhong Y, Wang J, Zhang R, Wei W, Wang H, Lu X, et al. Morphology-controlled self-assembly and synthesis of photocatalytic nanocrystals. *Nano Letters*. 2014;**14**:7175-7179. DOI: 10.1021/nl503761y
- [121] Wang J, Zhong Y, Wang L, Zhang N, Cao R, Bian K, et al. Morphology-controlled synthesis and metalation of porphyrin nanoparticles with enhanced photocatalytic performance. *Nano Letters*. 2016;**16**:6523-6528. DOI: 10.1021/acs.nanolett.6b03135
- [122] Mandal S, Nayak SK, Mallampalli S, Patra A. Surfactant-assisted porphyrin based hierarchical nano/micro assemblies and their efficient photocatalytic behavior. *ACS Applied Materials & Interfaces*. 2013;**6**:130-136. DOI: 10.1021/am403518d
- [123] La DD, Rananaware A, Salimimarand M, Bhosale SV. Well-dispersed assembled porphyrin nanorods on graphene for the enhanced photocatalytic performance. *ChemistrySelect*. 2016;**1**:4430-4434. DOI: 10.1002/slct.201601001

- [124] Tian Y, Martin KE, Shelnut JY-T, Evans L, Busani T, Miller JE, et al. Morphological families of self-assembled porphyrin structures and their photosensitization of hydrogen generation. *Chemical Communications*. 2011;**47**:6069-6071. DOI: 10.1039/C1CC10868A
- [125] Li C, Park K-M, Kim H-J. Ionic assembled hybrid nanoparticle consisting of tin (IV) porphyrin cations and polyoxomolybdate anions, and photocatalytic hydrogen production by its visible light sensitization. *Inorganic Chemistry Communications*. 2015;**60**:8-11. DOI: 10.1016/j.inoche.2015.07.016
- [126] Chen Y, Zhang C, Zhang X, Ou X, Zhang X. One-step growth of organic single-crystal p-n nano-heterojunctions with enhanced visible-light photocatalytic activity. *Chemical Communications*. 2013;**49**:9200-9202. DOI: 10.1039/C3CC45169K
- [127] Maiti NC, Mazumdar S, Periasamy N. J- and H-aggregates of porphyrin-surfactant complexes: Time-resolved fluorescence and other spectroscopic studies. *The Journal of Physical Chemistry B*. 1998;**102**:1528-1538. DOI: 10.1021/jp9723372
- [128] Marciniak H, Li X-Q, Wurthner F, Lochbrunner S. One-dimensional exciton diffusion in perylene bisimide aggregates. *The Journal of Physical Chemistry A*. 2010;**115**:648-654. DOI: 10.1021/jp107407p
- [129] Jurchescu OD, Baas J, Palstra TT. Effect of impurities on the mobility of single crystal pentacene. *Applied Physics Letters*. 2004;**84**:3061-3063. DOI: 10.1063/1.1704874
- [130] Takeya J, Yamagishi M, Tominari Y, Hirahara R, Nakazawa Y, Nishikawa T, et al. Very high-mobility organic single-crystal transistors with in-crystal conduction channels. *Applied Physics Letters*. 2007;**90**:102120. DOI: 10.1063/1.2711393
- [131] Zhong Y, Wang Z, Zhang R, Bai F, Wu H, Haddad R, et al. Interfacial self-assembly driven formation of hierarchically structured nanocrystals with photocatalytic activity. *ACS Nano*. 2014;**8**:827-833. DOI: 10.1021/nn405492d
- [132] Wang Z, Li Z, Medforth CJ, Shelnut JA. Self-assembly and self-metallization of porphyrin nanosheets. *Journal of the American Chemical Society*. 2007;**129**:2440-2441. DOI: 10.1021/ja068250o
- [133] Huang C-C, Parasuraman PS, Tsai H-C, Jhu J-J, Imae T. Synthesis and characterization of porphyrin-TiO<sub>2</sub> core-shell nanoparticles as visible light photocatalyst. *RSC Advances*. 2014;**4**:6540-6544. DOI: 10.1039/C3RA45492D
- [134] Chen Y, Li A, Jin M, Wang L-N, Huang Z-H. Inorganic nanotube/organic nanoparticle hybrids for enhanced photoelectrochemical properties. *Journal of Materials Science & Technology*. 2016. DOI: 10.1016/j.jmst.2016.08.030
- [135] Chen Y, Huang Z-H, Yue M, Kang F. Integrating porphyrin nanoparticles into a 2D graphene matrix for free-standing nanohybrid films with enhanced visible-light photocatalytic activity. *Nanoscale*. 2014;**6**:978-985. DOI: 10.1039/C3NR04908F
- [136] Guo P, Chen P, Liu M. One-dimensional porphyrin nanoassemblies assisted via graphene oxide: Sheetlike functional surfactant and enhanced photocatalytic behaviors. *ACS Applied Materials & Interfaces*. 2013;**5**:5336-5345. DOI: 10.1021/am401260n

- [137] Wang D, Pan J, Li H, Liu J, Wang Y, Kang L, et al. A pure organic heterostructure of  $\mu$ -oxo dimeric iron (iii) porphyrin and graphitic- $C_3N_4$  for solar  $H_2$  reduction from water. *Journal of Materials Chemistry A*. 2016;**4**:290-296. DOI: 10.1039/C5TA07278F
- [138] Ling MM, Bao Z. Thin film deposition, patterning, and printing in organic thin film transistors. *Chemistry of Materials*. 2004;**16**:4824-4840. DOI: 10.1021/cm0496117
- [139] Zhang X, Jie J, Deng W, Shang Q, Wang J, Wang H, et al. Alignment and patterning of ordered small-molecule organic semiconductor micro-/nanocrystals for device applications. *Advanced Materials*. 2016;**28**:2475-2503. DOI: 10.1002/adma.201504206
- [140] Kira A, Tanaka M, Umeyama T, Matano Y, Yoshimoto N, Zhang Y, et al. Hydrogen-bonding effects on film structure and photoelectrochemical properties of porphyrin and fullerene composites on nanostructured  $TiO_2$  electrodes. *The Journal of Physical Chemistry C*. 2007;**111**:13618-13626. DOI: 10.1021/jp0726079
- [141] Nagai K, Abe T, Kaneyasu Y, Yasuda Y, Kimishima I, Iyoda T, et al. A full-spectrum visible-light-responsive organophotocatalyst film for removal of trimethylamine. *ChemSusChem*. 2011;**4**:727-730. DOI: 10.1002/cssc.201100064
- [142] Abe T, Tobinai S, Taira N, Chiba J, Itoh T, Nagai K. Molecular hydrogen evolution by organic p/n bilayer film of phthalocyanine/fullerene in the entire visible-light energy region. *The Journal of Physical Chemistry C*. 2011;**115**:7701-7705. DOI: 10.1021/jp1094992
- [143] Imahori H, Norieda H, Nishimura Y, Yamazaki I, Higuchi K, Kato N, et al. Chain length effect on the structure and photoelectrochemical properties of self-assembled monolayers of porphyrins on gold electrodes. *The Journal of Physical Chemistry B*. 2000;**104**:1253-1260. DOI: 10.1021/jp992768f
- [144] Imahori H, Yamada H, Ozawa S, Sakata Y, Ushida K. Synthesis and photoelectrochemical properties of a self-assembled monolayer of a ferrocene-porphyrin-fullerene triad on a gold electrode. *Chemical Communications*. 1999:1165-1166. DOI: 10.1039/A903237A
- [145] Imahori H, Fujimoto A, Kang S, Hotta H, Yoshida K, Umeyama T, et al. Molecular photoelectrochemical devices: Supramolecular incorporation of  $C_{60}$  molecules into tailored holes on porphyrin-modified gold nanoclusters. *Advanced Materials*. 2005;**17**:1727-1730. DOI: 10.1002/adma.200401770
- [146] Imahori H, Hasobe T, Yamada H, Nishimura Y, Yamazaki I, Fukuzumi S. Concentration effects of porphyrin monolayers on the structure and photoelectrochemical properties of mixed self-assembled monolayers of porphyrin and alkanethiol on gold electrodes. *Langmuir*. 2001;**17**:4925-4931. DOI: 10.1021/la010006h
- [147] Abe T, Tanno Y, Ebina T, Miyakushi S, Nagai K. Enhanced photoanodic output at an organic p/n bilayer in the water phase by means of the formation of whiskered phthalocyanine. *ACS Applied Materials & Interfaces*. 2013;**5**:1248-1253. DOI: 10.1021/am302209b

- [148] Sandanayaka AS, Murakami T, Hasobe T. Preparation and photophysical and photoelectrochemical properties of supramolecular porphyrin nanorods structurally controlled by encapsulated fullerene derivatives. *The Journal of Physical Chemistry C*. 2009;**113**:18369-18378. DOI: 10.1021/jp9063577
- [149] Klauk H, Halik M, Zschieschang U, Eder F, Schmid G, Dehm C. Pentacene organic transistors and ring oscillators on glass and on flexible polymeric substrates. *Applied Physics Letters*. 2003;**82**:4175-4177. DOI: 10.1063/1.1579870
- [150] Gustafsson G, Cao Y, Treacy G, Klavetter F, Colaneri N, Heeger A. Flexible light emitting diode. *Nature*. 1992;**357**:477

IntechOpen

